CoA Note No. 106

THE COLLEGE OF AERONAUTICS

CRANFIELD

LOW SPEED WIND TUNNEL TESTS ON A 70° CROPPED DELTA WING

by

A. J. ALEXANDER

NOTE NO. 106

September, 1960

THE COLLEGE OF AERONAUTICS

CRANFIELD

Preliminary Low Speed Wind Tunnel Tests on a 70° Cropped Delta Wing with Blowing at all Edges *

- by -

A. J. Alexander, M.Sc., A.F.R.Ae.S.

SUMMARY

Wind tunnel tests have been made on a 70° Cropped Delta Wing with slot blowing from all edges in the plane of the wing. The tests include six-component force and moment measurements and the distribution of pressure at four chordwise stations on the upper surface. Some results are also given with slot blowing from one wing-tip.

At a constant incidence blowing increases the size and strength of the leading edge vortices and moves the vortex cores outboard. It also eliminates the secondary separation. Extra non-linear lift is obtained from the increased vortex strength and the lift coefficient at $\alpha = 25^{\circ}$ is increased from 0.98 without blowing to 1.16 and 1.25 for C_{μ} values of 0.123 and 0.278 respectively with blowing from all edges. The corresponding movement of the centre of pressure is less than one per cent of the root chord.

If allowance is made for the wind-off jet drag due to the poor blowing distribution, the values of drag obtained with blowing at all edges are lower than those for the unblown case at a given lift and the resultant lift-to-drag ratios are much improved. Without blowing the maximum ratio is 6.5 at a C_L of 0.13 but blowing from all edges with C_{μ}'s of 0.123 and 0.278 increases this value to 13.8 and 18.7 respectively at approximately the same lift coefficient.

At incidence, with blowing at all edges, the jet sheets roll up to form stable leading edge vortices but near zero incidence ($\alpha < 0.25^{\circ}$) the jet sheets oscillate from one surface to the other, due to a downwash lag effect, producing a sinusoidal lift.

---

* This work has been partly supported by Ministry of Aviation Contract No. PD/28/02 and will form part of the author's Ph.D. Thesis to be presented in August, 1961. It is given limited advanced circulation under the terms of the contract but no reference may be made to it before publication of the thesis.

CONTENTS

LIST OF SYMBOLS

α	Geometric wing incidence
β	Angle of sideslip
b	Wing span = 1.62 ft.
c_o	Root chord = 3.33 ft.
$\bar{c}$	Aerodynamic mean chord $= \dfrac{\int_{-b/2}^{b/2} c^2 \, dy}{\int_{-b/2}^{b/2} c \, dy} = 2.60$ ft.
m_j	Jet mass flow
v_j	Average final jet velocity assuming isentropic expansion to free stream static pressure. (See para. 2)
q_o, U_o, p_o, M_o	Mainstream dynamic pressure, velocity and pressure and Mach No.
p	Static pressure
s	Wing semi-span
x, y, z	Body axes (see Fig. 7)
$x_{C.P.}$	Distance of centre of pressure from apex
x′	Distance from apex
A	Wing aspect ratio = 0.73
Re	Reynolds number based on aerodynamic mean chord
S	Wing area = 3.60 sq. ft.
C_p	Static pressure coefficient $= \dfrac{p - p_o}{q_o}$
C_μ	Blowing momentum coefficient $= \dfrac{m_j v_j}{q_o S}$

List of Symbols (Continued)

C_L Lift coefficient $= \frac{\text{Lift}}{q_o S}$

C_D Drag coefficient $= \frac{\text{Drag}}{q_o S}$

C_D^* $C_D - C_{Dj}$ (see para. 4.2)

C_{Dj} $\frac{\text{(Jet drag, wind off)}}{q_o S}$

C_c Cross-wind force coefficient $= \frac{\text{Crosswind force}}{q_o S}$

C_l Rolling moment coefficient $= \frac{\text{R.M.}}{q_o S\, b}$

C_m^* Pitching moment coefficient about aerodynamic mean quarter chord ($0.415\, C_o$) $= \frac{\text{P.M.}}{q_o S\, \bar{c}}$

C_n^* Yawing moment coefficient about aerodynamic mean quarter chord $= \frac{\text{Y.M}}{q_o S\, b}$

1. Introduction

The slender wings suitable for supersonic flight have, in general, both low lift to drag ratios and lift curve slopes. The former is a disadvantage in the cruise condition and the latter during take-off and landing. This loss of lift with decreasing aspect ratio has been predicted by the various theories which assume attached flow, see for example Ref. 1. The picture is complicated however by the fact that in practice the flow is very largely three dimensional and includes regions of separation. In particular powerful leading edge or tip vortices are formed depending on the wing plan-form.

These viscous effects are not necessarily undesirable since they result in large increases in the lift curve slope, Ref. 2 and thus improve the lowspeed performance. With highly swept wings however, separation from sharp leading edges means a loss of suction there with an increase in drag and consequent reduction of the lift to drag ratio. This is offset to some extent by the increased lift.

Some attempts have been made to improve the low speed performance of low aspect ratio delta wings using methods that have proved successful on high aspect ratio unswept wings. Tests have been made using plain round-nosed flaps both with and without boundary layer control and also using jet flaps. (Refs. 3,4). Considerable increases in lift were obtained but the rather large movement of the centre of pressure might prove difficult to trim.

Since the leading edge vortices, or tip vortices in the case of unswept wings, play such an important part in determining the flow pattern it would seem desirable to exercise some means of control over their development and still further increase their favourable influence. In order to achieve this, tests have been made using thin high velocity jet sheets emitted from slots in the wing-tip of both a low aspect ratio unswept wing, Ref. 5, and a 40^{o} swept wing, Ref. 6.

In both sets of tests spanwise blowing resulted in increased lift. The effect of the blowing on the unswept wing was to change the spanwise lift distribution from near elliptic to approximately constant loading as the ability of the jet sheet to support a pressure difference increased the loading near the tips. Also the trailing vortex was moved some distance outboard. With the swept wing spanwise blowing increased the size and strength of the leading edge vortex and moved it outboard. In this case also the increase in lift was mainly due to an increase in the loading of the outer sections of the wing. The increase in lift was

obtained with little change in the longitudinal static stability over the greater part of the usable C_L range.

In the case of the highly swept delta wing with sharp leading edges, separation occurs along the whole leading edge with the wing at incidence. Neglecting the upstream effect of the trailing edge the flow over the wing is conical, the leading edge vortices growing linearly with distance from the apex. The effect of leading edge blowing will be to increase the size and strength of the leading edge vortices, and, if the blowing slot were triangular (i.e. increasing in width linearly from the apex), this would be possible without changing the conical nature of the flow and hence without changing the trim. Some wind tunnel tests made at the Royal Aircraft Establishment on 70° swept delta wings with leading edge blowing support the hypothesis that a triangular slot is suitable for this planform.

Since it is possible to control the leading edges vortices by the leading edge blowing it may be possible, by means of differential blowing, to exercise control both in roll and yaw without a corresponding change in trim. Similarly the static stability of the aircraft might be changed, and in particular, reductions in the magnitude of l_v (rolling moment due to sideslip) at high lift coefficients would be very useful.

A disadvantage of blowing from a swept leading edge is the increase in drag due to the forward component of thrust. To overcome this difficulty it was decided to eject the air at an angle to the edge in a rearward direction and thus obtain an increment in thrust without seriously modifying the effect on the leading edge vortices. The present tests however were made using a slot of constant width with air ejection normal to the edge, and were designed to provide a basis for comparison with later tests using directed blowing.

The cropped delta planform used in these tests was chosen for two reasons, (a) it has a lower vortex drag for a given value of the slenderness parameter $\frac{(M_o^2 - 1)s}{c_o}$, and (b) the in-line tips should enable a larger thrust component to be obtained from the edge blowing (Ref. 7). Trailing edgeblowing was also incorporated to increase the thrust and to increase the lift at low speeds by preventing the loss of lift near the trailing edge.

2. Model and Experimental Method

The model is shown in Figs. 1 and 4. It is a 70^{o} swept delta wing with cropped tips, of chord equal to one third of the root chord, and has an aspect ratio of 0.73. The main body is a hollow gunmetal casting and detachable brass edges form a continuous blowing slot round the periphery (of constant width 0.040 ins.) except for a small region near the apex. The model is of rhombic cross-section, the total edge angle on both leading edge and tips is 20^{o} whilst the trailing edge angle is 15^{o}.

Pressure plotting stations were located at 0.33 c_o, 0.49 c_o, 0.63 c_o and 0.87 c_o from the apex and consisted of two continuous tubes each spanning half of the wing. Thirty-six static pressure holes were drilled at each station to enable the spanwise pressure distribution to be accurately described.

The tests were made in the College of Aeronautics 8ft x 6ft low speed wind tunnel with the model supported on a Warden type six-component balance. High pressure air was fed to the model at the balance virtual centre through the hollow support strut, and constraints were kept to a minimum by the use of a flexible circular ring-main feed, see Fig. 3.

The mass flow of air to the model, m_j, was measured by orifice plates in the main feed pipe. The pressure distribution in the slot was measured with a total head tube and the theoretical jet velocity was calculated assuming isentropic expansion to free stream pressure. Owing to the variation of velocity along the slot, see Fig. 8, the calculation of C_μ in the normal way was not possible. An average constant velocity, v_j, giving the same total mass flow, was computed from the velocity distribution. C_μ was then defined as $C_\mu = \frac{m_j v_j}{q_o S}$

3. Balance measurements

In all the tests six component balance measurements were made. In this report forces are referred to wind axes and moments to body axes, see Fig. 7. Conversion of the moments from wind axes to body axes was made using the following formulae :-

$$C_l = C'_l \cos\beta \cos\alpha - \frac{\bar{c}}{b} C'_m \sin\beta \cos\alpha - C'_n \sin\alpha$$

$$C_m = C'_m \cos\beta + \frac{b}{\bar{c}} C'_l \sin\beta$$

$$C_n = C'_n \cos\alpha + C'_l \cos\beta \sin\alpha - \frac{\bar{c}}{b} C'_m \sin\beta \sin\alpha$$

where the dashes denote measured moments relative to wind axes. Pitching and Yawing moments are referred to the aerodynamic mean quarter chord point by the formulae :-

$$C^*_m = C_m - \frac{a}{\bar{c}} \left[C_L \cos\alpha + C_D \cos\beta \sin\alpha - C_c \sin\beta \sin\alpha \right]$$

$$C^*_n = C_n + \frac{a}{b} \left[C_c \cos\beta + C_D \sin\beta \cos\alpha - C_L \sin\alpha \sin\beta \right]$$

where a is the distance from the pivot point to the aerodynamic mean quarter chord point. In tests with blowing the high pressure air caused the flexible ring main to distort slightly and this induced additional forces and moments. To correct for these changes the model was removed periodically and a calibrator (see Fig. 2) was attached to the balance strut. The calibrator consisted of a short length of pipe feeding air to the adjustable gap between two flanges. The gap was set such that with any given model configuration the mass flow was the same for a fixed control pressure. Since the air was emitted radially from the virtual centre of the balance the only forces and moments present should be those due to the distortion of the ring main. In order to allow for the slight inaccuracies in manufacture the balance measurements were taken with the calibrator in a fixed position and then rotated through 180^o. The average of the two sets of readings was taken to be the balance constraint correction due to blowing. Balance constraint corrections due to blowing for a control pressure of 30 p.s.i. gauge at the orifice plates (C_μ = .278) with the whole slot open are given below (based on $q_o S$ with U_o = 100 f.p.s.) :-

Lift	- .41 lb.	C_L	- .009
Drag	- .09 lb.	C_D	- .002
Cross Wind force	+ .63 lb.	C_c	+ .015
Rolling moment	+ 1.91 lb. ft.	C'_l	+ .027
Pitching moment	+ .46 lb. ft.	C'_m	+ .004
Yawing moment	+ 2.10 lb. ft.	C'_n	+ .030

The moments here are referred to the balance virtual centre and wind axes.

Overall accuracy of coefficients (moments referred to body axes. See list of symbols).

C_L	±	.002
C_D	±	.0002
C_c	±	.002
C_l	±	.002
C^*_m	±	.001
C^*_n	±	.002

Wind tunnel corrections have not been applied to the present results since no suitable corrections are available but conventional corrections are small, $\Delta\alpha = 0.5^o$ for $\alpha = 25^o$ and $\Delta C_D = .009$ for $C_D = 0.45$. Corrections have been applied to C_D, C^*_m, C^*_n to allow for the drag of the incidence wire and the small exposed part of the main feed pipe.

4. Discussion of results

Before commencing the main wind tunnel programme some preliminary tests were made with and without blowing from all edges over a range of wind-speeds. These tests were designed (1) to find the effect of varying Reynolds number, (2) to find the maximum value of C_μ, which was lower than anticipated due to losses in the system, and (3) to find the magnitude of the balance constraints due to blowing.

Wind speed was varied between 50 ft/sec. and 200 ft/sec. both with and without blowing and no appreciable Reynolds number effect was observed. Hence the tests without blowing were made at the maximum

speed of 200 ft/sec. to obtain the greatest accuracy but the tests with blowing were made at lower wind speeds in order to achieve reasonable values of C_μ. A few tests were made at a wind speed of 50 ft/sec. with a maximum C_μ value of 1.05, but balance readings were less accurate at this low speed and the remainder of the tests with blowing were made at 100 ft/sec. when the maximum value of C_μ was 0.28.

Although the balance constraint corrections to rolling and yawing moment were comparatively large the accuracy of measurement and repeatability were such that the overall accuracy was quite acceptable (see paragraph 3).

Comparative tests were made without blowing (a) with the slot open and (b) sealed to prevent any airflow through the slot. Sealing the slot did not change lift, drag, cross-wind force or pitching moment appreciably but large changes in rolling and yawing moments occurred at high incidence.

If edge blowing were to be used as a control some form of asymmetric blowing would be necessary. Apart from the cases without blowing and with blowing from all edges, four other blowing configurations were tested as follows :-

(1) Blowing from one tip only
(2) Blowing from one tip and the whole trailing edge
(3) Blowing from one leading edge and tip only
(4) Blowing from one leading edge, tip and the whole trailing edge.

These tests were designed to show the effects of asymmetric blowing and also the effect of using a trailing edge jet sheet in conjunction with blowing from swept and streamwise edges. Six-component balance measurements were made for all blowing configurations. As the test results with the various forms of asymmetric blowing were not dissimilar only the results with tip blowing are presented here. The effects of trailing edge blowing could not be clearly ascertained as losses in the system greatly reduced the amount of air ejected from the trailing edge.

4.1. Lift

The jet sheet originating from the leading edge and tips rolls up to form the leading edge vortex in a manner similar to the rolling up of the free vortex sheets without blowing although the pressure boundary condition is changed since the jet sheet can now support a pressure difference. This rolling up of the jet sheet has occurred in all the reported tests using edge blowing from swept-back or streamwise tips and is a stable type of flow. A sharp change in lift and pitching moment occurs however on passing through zero incidence when the vortex so formed moves from one surface to the other. This can be seen in Fig. 9 where both the lift and pitching moment exhibit discontinuities near zero incidence. There was no abrupt change in the other forces and moments in this region.

In the tests near zero incidence with blowing at all edges it was possible to find an incidence where the leading edge and tip jet sheets oscillated from one surface to the other producing a sinusoidal lift. The frequency of the oscillation was about one cycle per second and is thought to be associated with downwash lag in the following manner. Only a very small positive incidence ($<0.25^{\circ}$) is sufficient to ensure that the jet sheet rolls up over the wing upper surface, thus producing (for the values of C_{μ} used in the present tests) values of C_L of 0.02 or greater, i.e. at least four times the lift produced by the wing without blowing at the same incidence. This lift is sufficient to produce a downwash on the wing of at least 0.5° ($\epsilon \simeq \frac{C_L}{\pi A}$) which is greater than the geometric incidence. Consequently the wing is now at an effective incidence of -0.25°, sufficient to induce the vortices to move to the other surface. Thus an oscillating motion is set up which would be undesirable in an aircraft although it seems unlikely that this condition would be approached in practice.

Lift-incidence curves are shown in Figs. 10 to 12. Without blowing the graphs exhibit the usual non-linear slope although near zero incidence they follow closely the R. T. Jones value for attached flow. At $\alpha = 25^{\circ}$ the non-linear lift is equal to the linear contribution. In no case is the effect of sideslip significant.

The effect of edge blowing, for all configurations tested, was to increase the lift at constant incidence. Since blowing increases the size and strength of the leading edge vortices it increases mainly the non-linear lift but its effect is felt on the whole upper surface pressure

distribution (see paragraph 4.7). Fig. 11 shows the effect of blowing from all edges and Fig. 12 gives results obtained with blowing from one wing-tip. Lift increases were obtained, with blowing, over the whole incidence range and the lift increments increased with incidence which is consistent with the observation that blowing affects mainly the non-linear lift due to its effect on the leading edge vortices. At the higher incidences some lift magnification was obtained ($\Delta C_L > C_\mu$) except for the larger C_μ value with blowing from all edges. For instance at $\alpha = 25^o$, $\Delta C_L = 0.18$ for a C_μ value of 0.123 with blowing from all edges and $\Delta C_L = 0.12$ for $C_\mu = 0.060$ with blowing from one wing-tip.

Fig. 13, which includes some points obtained in early tests, shows the increase in lift with momentum coefficient C_μ at constant incidence with blowing at all edges. The increase is similar in form to that obtained with a wing having blowing boundary layer control on a deflected flap, i.e. an initial steep rise in lift followed by a more gradual increase. In this case however the increase is due rather to slow changes in the flow pattern without essentially changing its form, rather than the large changes which occur when flow separation over the deflected flaps is suppressed. The initial increase in lift is due to an increase in the vortex strength while the vortex core remains over the wing. Tuft observations, however, show that for much larger values of C_μ the vortex core moves off the wing surface; for instance at a C_μ of 1.0 the sweep of the vortex core is about 65^o compared with a leading edge sweep of 70^o, with a corresponding drop in the rate of increase of lift with increase of C_μ .

Although blowing increased the lift on all configurations tested it was difficult to ascertain the effect of trailing edge blowing as the amount of air emitted at the trailing edge was only about half the calculated amount due to pressure losses in the system*. It is also difficult to predict at this stage the best configuration for increasing lift but further tests are planned using directed blowing and lower values of C_μ.

---

* Modifications have now been made to reduce these losses.

4.2. Drag

Drag is plotted against lift in Figs. 14 to 16. Fig. 14 shows the results obtained without blowing and the effect of sealing the slot which was small. Sideslipping the model between $\pm 5^{o}$ had a negligible effect on the drag and this was also the case with all the blowing configurations tested.

It has been observed in some tests, e.g. Ref. 8, that there is a dip in the drag curve near zero lift due to the formation of areas of laminar flow. No such effect has been observed in the present tests and the minimum drag value of 0.011 is sufficiently close to the estimated turbulent value (skin friction + L.E. form drag) of 0.0092 to indicate that the flow was turbulent at all times although no special effort was made to fix transition.

Tests with blowing at all edges, Fig. 15, showed large increases in the zero lift drag. Ideally, with the constant-width open slot configuration tested (excluding the small region near the apex) and with constant slot pressure there would have been no net thrust on the model due to the jet. Fig. 8 shows that this ideal situation was not realised due to the inadequate trailing edge blowing and a net drag was sustained as a result. Of the two curves plotted for each C_{μ} in Fig. 15 the upper curve is the total drag of the model as measured on the balance. The lower curve was obtained by subtracting from the total measured drag the jet drag (direct jet thrust) wind-off due to blowing from all edges.

This lower curve shows that the aerodynamic effect of blowing from all edges is beneficial and the drag for a given lift is less than for the unblown case over the whole incidence range. The greater reductions in drag at the higher incidences are due to the lower induced drag component.

With blowing from the starboard tip a small amount of thrust recovery was obtained but did not exceed 10% of the theoretical C_{μ} value. At higher incidence the drag was close to that obtained by blowing from all edges at the same value of C_{μ} .

Fig. 17 gives lift to drag ratios without blowing and with blowing from all edges. In Fig. 17a the unblown case is compared with the blown case using the drag values as measured by the balance. The low lift to drag ratios obtained are due entirely to the large zero-lift drag values. This also causes the maximum lift to drag ratio to occur

at higher values of lift with blowing. The values obtained without blowing correspond reasonably well with the delta wing results of Ref. 9.

For a flat plate delta wing with leading edge separation (no nose suction) the induced drag will be L tan α and the corresponding lift to drag ratio (excluding skin friction) is cot α. This is also plotted in Fig. 17a using the lift values obtained without blowing. At higher incidences ($C_L > 0.5$) the lift to drag ratio exceeds the value cot α for all cases due to the suction forces acting on the forward facing surfaces.

In Fig. 17b the values of lift to drag ratio, for blowing at all edges, obtained using the lower curves of Fig. 15 are again compared with the unblown case and the inviscid value cot α. In this case blowing from all edges improves the lift to drag ratio considerably and exceeds the value of cot α for lift coefficients as low as 0.1. The maximum value without blowing of 6.5 at a C_L of 0.13 is increased, with blowing at all edges, to 13.8 and 18.7 for C_μ values of 0.123 and 0.278 at C_L's of 0.11 and 0.14 respectively.

4.3. Cross-wind force

Cross-wind force is plotted against the sideslip angle β in Figs. 18 to 20. In the range of sideslip tested ($-5^\circ \leq \beta \leq +5^\circ$) the variation is a linear one. This was the case in all the present tests. The results with blowing from all edges are little changed from the unblown case, apart from a small crosswind force at zero sideslip due to asymmetrics in the blowing.

With blowing from one tip only there is a large crosswind force at zero sideslip due to the jet momentum in the crosswind direction. This value is close to the theoretical momentum coefficient C_μ at small incidence and provides a useful check on the method of estimating C_μ. The graph is now no longer symmetrical about zero sideslip. The tip jet rolls up to form a strong vortex and the crosswind force due to the resultant increased suctions on that section of the wing oppose the jet reaction.

However, the value of $\frac{\partial C_c}{\partial \beta}$ was little changed by any of the forms of blowing tested and it seems unlikely that this type of blowing, i.e. edge jets, will affect the stability.

4.4. Pitching moments

The pitching moment about the aerodynamic mean quarter-chord point is plotted against lift in Figs. 21 to 23. Without blowing and with an open slot the points lie on a straight line but with the slot sealed the curve is slightly non-linear, the aerodynamic centre moving back by about 1% of the root chord compared with the slot open case at a C_L of 1.0. Sideslipping up to $\pm 5^o$ produced no change of pitching moment.

With blowing from all edges there was a sudden change in the pitching moment near zero incidence, this can be clearly seen in Fig. 9, caused by the vortex moving from one surface to the other. Away from zero incidence however the flow pattern was quite stable and the overall effect of the blowing was to change the pitching moment at zero lift $C^*_{m_o}$ but there was only a slight change in the position of the aerodynamic centre. Blowing from the wing tip also increased $C^*_{m_o}$ and moved the aerodynamic centre rearwards, i.e. the wing became more stable in pitch.

The movement of the centre of pressure is shown in Fig. 24. Without blowing there is little movement above a C_L of 0.4 while for C_L values as low as 0.10 the centre of pressure moves forward only about 2% of the root chord.

When blowing from all edges, too much air is ejected from the leading edge, see Fig. 8, with the result that the lift increase on the forward part of the wing is proportionately greater than that obtained further back, thus causing a forward movement of the centre of pressure especially at low incidence. A suitable form of tapered blowing (see paragraph 1), should maintain conical flow and increase the lift without a corresponding change in the position of the centre of pressure*. Tapered blowing should reduce the values of C_μ required for a given lift due to a more efficient use of the air available.

With tip blowing the centre of pressure moves aft due to the increased load near the tips. In this case the movement of the centre of pressure is small for C_L's above 0.3 but below this value it moves aft rapidly as the majority of the lift is then being produced by the action of the tip jet.

---

* Suitable modifications are in hand using the edge slots of Fig. 5.

4.5. Rolling moments

In Figs. 25 to 27 the rolling moment about model centre line is plotted against sideslip angle β and the corresponding slopes $l_v \left(\equiv \frac{\partial C_l}{\partial \beta} \right)$ are plotted against lift in Figs. 28 to 30. The variation of C_l is linear within the range $-5^o \leqslant \beta \leqslant +5^o$.

The rolling moments induced on a delta wing in sideslip are due to an asymmetric pattern of the leading edge vortices, Ref.9. The vortex on the advancing edge remains tightly rolled but that on the retreating edge becomes more diffuse and weaker. Thus for negative sideslip there is a positive rolling moment, i.e. l_v is negative and increases in magnitude with increase of incidence due to the increased non-linear lift. These trends are clear from Figs. 25 & 28 without blowing. Only at the highest incidence is there an appreciable difference due to sealing the slot.

Without blowing the rolling moment due to sideslip is mainly due to a weakening of the leading edge vortex on the retreating edge. With blowing, however, the rolling up of the leading edge vortices is partly controlled by the jet sheet which would be comparatively unaffected by sideslip and would tend to strengthen the vortex on the retreating leading edge.

This would reduce the magnitude of C_l and hence l_v at a given incidence. From the results however it appears that this is only true at higher incidence, Fig. 9 shows that l_v is reduced with blowing from all edges above a C_L of 0.5.

Figs. 27 and 30 show the effect of blowing from one wing tip only. Although the values of l_v are very close to the unblown case the asymmetric blowing produces substantial rolling moments at zero sideslip and should be capable of trimming 4^o of sideslip up to high incidence. Unfortunately doubling the amount of blowing scarcely improves this.

4.6. Yawing moments

Yawing moments about aerodynamic mean quarter chord are plotted against sideslip angle β in Figs. 31 to 33 and the slopes $n_v \left(\equiv \frac{\partial C_n}{\partial \beta}\right)$ plotted against lift in Figs. 34 to 36. In all the tests the variation of yawing moment with sideslip angle was approximately linear in the range tested ($-5^o \leqslant \beta \leqslant +5^o$). Without blowing the asymmetric pressure distribution due to sideslip (see paragraph 4.5) will produce a yawing moment on a wing with thickness due to the pressure differential on the vertical surfaces. The effect of sealing the slot is small at low incidence but becomes appreciable above $\alpha = 10^o$. The pressure distributions indicate a considerable pressure change along the slot and without sealing this would produce an airflow in the slot towards the apex, thus increasing the pressure there. Although this would occur on both leading edges, when the wing was side-slipping the effect would be most marked on the advancing leading edge (see paragraph 4.5). This increase of pressure in the slot towards the apex would increase the magnitude of the yawing moment particularly at high incidence when the pressure gradient along the slot is greatest. This effect can be clearly seen in Figs. 31 and 34.

The change of yawing moment with sideslip angle is not greatly affected by blowing but $C^*_{n_o}$ has a non-zero value given by the yawing moment produced by the direct jet thrust which in turn depends on the blowing configuration. True asymmetric blowing configurations, such as blowing from one wing-tip, Fig. 33, produce large values of $C^*_{n_o}$ but with blowing from all edges the non-zero value of $C^*_{n_o}$ is due to irregularities in the slot pressure distribution.

4.7. Upper surface static pressures

The spanwise variation of static pressure was measured at four chordwise stations, 0.33 C_o, 0.49 C_o, 0.63 C_o and 0.87 C_o at zero sideslip for a range of incidence $\alpha = 2^o$, 5^o, 10^o, 15^o, 20^o, 25^o and C_μ values of 0, 0.123 and 0.278 with blowing at all edges. This is shown in Figs. 37 to 48. The pressures on the starboard side are on the left in the figures, i.e. the wing is viewed from the stream direction.

Without blowing the pressure distributions are typical of wings with sharp, highly swept leading edges. The suction peak which occurs beneath the vortex core can be clearly seen particularly at the more forward stations and small suction peaks are evident at angles of incidence as low as 2^{o}. At higher incidence the secondary separation, due to the adverse pressure gradient near the leading edge is manifest by a region of roughly constant pressure outboard of the main vortex core. Reasonable agreement is obtained with the results of Ref. 10 in which surface static pressures were measured on a 70^{o} true delta wing.

The flow may be said to remain conical back to at least 65% of the root chord, i.e. back to the leading edge-tip junction see Figs. 37, 40, 43. In subsonic flow the lift falls over the rear part of the wing due to the requirement of zero load at the trailing edge. This is clear from Fig. 46 which shows the pressure distribution at 87% of the root chord. The reduction in lift over the rear part of the wing is somewhat greater in the present case than for the comparable delta wing of Ref. 10. This is probably due to the effect of the streamwise tips, for, according to the R. T. Jones theory for attached flow this rear part of the wing would produce no lift at all.

With edge blowing the leading edge vortices are increased in strength due to the higher rate at which vorticity is shed from the leading edges and in size due to the change in the pressure boundary condition. The increase in vortex strength is shown by the larger suction peaks obtained on the wing upper surface with blowing, see Figs. 37 and 38. The asymmetry is due to differences in slot width. The increase in vortex size results from the ability of the jet sheet to support a pressure difference whereas for the free vortex sheet (without blowing) the boundary condition is that the pressure change across the sheet is zero. Initially, at least, the boundary condition will be of the type applicable to thin curved jets, i.e.

$$\Delta p = \frac{\delta \rho V^2}{R} \qquad (1)$$

where R is the radius of curvature of the jet sheet.
This may be re-written :

$$-C_p = \frac{C_\mu . S}{R} \quad \text{or} \quad -C_p \propto \frac{C_\mu}{R} \qquad (2)$$

No pressure measurements were made across the jet but the value of C_p nearest to the edge may be taken as indicative of the trend and

and comparing Figs. 38 and 39 it can be seen that while C_μ is more than doubled the rise in $-C_p$ is much smaller.

Thus the value of R must increase to compensate for this change. Tuft observations confirm that the vortex increases in size and indicate that the circumferential velocities increase.

Blowing also moves the vortex cores outboard, for example at $\alpha = 25^o$ the spanwise movement of the vortex due to blowing is 15% of the semi-span, see Figs. 37 and 38. At much larger values of C_μ the vortex core moves right off the wing surface. Tuft observations show that for a C_μ value of 1.0 the sweep of the leading edge vortex core is only about 65^o compared with the leading edge sweep of 70^o. Tufts also indicate that the height of the vortex core above the wing increases with increasing C_μ. The movement of the vortex core is accomplished in two stages. Firstly, at a comparatively low value of C_μ (< 0.1) the entrainment effect of the jet is sufficient to eliminate the secondary vortex. Comparison of Figs. 37 and 38 shows that the constant pressure region outboard of the vortex core has disappeared with blowing. Without blowing the air flowing outwards under the vortex core cannot continue to move in a spanwise direction indefinitely because of the presence of the vortex sheet which springs from the leading edge. The effect of this build-up of air in the region near the leading edge is felt further back and the cross flow separates and flows away in a chordwise direction. With blowing the cross-flow is entrained by the jet sheet and no build-up occurs near the leading edge. Thus the cross-flow can negotiate this region without separation despite the larger adverse pressure gradient. Thus the initial movement of the vortex core is due to the removal of the secondary separation and the consequent reduction of pressure in that region and for moderate increases in C_μ the core position is little changed despite the increase in the size of the vortex, see Figs. 39, 39. At much larger values of C_μ, however, equation 2 indicates that the radius of the jet sheet must also increase considerably and eventually the rolling up occurs outboard of the leading edge. This is confirmed by tuft observations.

With blowing from all edges the conical nature of the flow is disturbed by the poor blowing distributions, since far too much air is ejected near the apex, see for example Figs. 38, 41, 44. Also the trailing edge blowing was small and ineffective and further emphasised the unbalanced blowing distribution. The amount of air emitted from the tips was of the right order but Figs. 47 and 48 show that blowing from the streamwise edges was much less effective than

leading edge blowing. A more powerful trailing edge jet might increase the effectiveness of the tip jets as the zero load condition at the trailing edge would no longer apply. This would automatically increase the loading along the tips and it is clear that edge blowing is most effective when applied to a region where a powerful vortex already exists.

Fig. 49 compares the upper surface pressure distribution at 0.33 C_o and 25° incidence both with and without blowing at all edges with the corresponding theoretical values of Mangler and Smith for the unblown case. The change in pressure distribution is not large for the two blowing cases considered and the vortex core position corresponds almost exactly with that predicted theoretically for the unblown case with no secondary vortex. Thus it seems fairly certain that the movement of the vortex core with blowing is due, initially at least, to the removal of the secondary separation and that the various theories fail to predict the position of the vortex core simply because the secondary separation is not included in the mathematical model. This conclusion is not new but is based here on experimental evidence which seems fairly conclusive.

Although the blowing case cannot strictly be compared with the unblown theoretical model it is interesting to note that while removal of the secondary vortex moves the main vortex core outboard the area of the wing affected by the main vortex is little changed from the unblown case with secondary separation and is much larger than that predicted theoretically. That this cannot be entirely due to the blowing can be seen from the fact that with C_μ = .123 slightly more of the wing pressure distribution is affected than for C_μ = .278. This suggests that the entrainment effects of the leading edge vortices exert a considerable influence on the upper surface distribution and that a satisfactory theory must include the effects of viscosity.

5. Conclusions

Low speed wind tunnel tests have been made to investigate the effect of slot blowing at all edges from a 70° Cropped Delta Wing.

The main conclusions are :

1. Blowing from the leading edge and tips increases the lift by increasing the size and strength of the leading edge vortices, i.e. the increase in lift is mainly due to an increase in the non-linear contribution.

2. The plane jet sheets issuing from the swept leading edges or streamwise tips roll up to form leading edge or tip vortices giving stable flow patterns with the wing at incidence. Close to zero incidence, however, the jet sheet oscillated from one surface to the other due to a downwash lag effect, producing a sinusoidal lift. This effect occurred only for incidences of less than 0.25° and seems unlikely to be a practical limitation.

3. In the present tests the leading edge blowing velocity distribution was unsatisfactory and too much air was emitted near the apex. With an improved distribution it should be possible to increase the lift without changing the conical nature of the flow, i.e. without changing the trim.

4. With blowing from all edges the lift to drag ratios calculated directly from the balance readings are low due to the poor blowing distributions which produce a net drag wind-off. When an allowance is made for this direct jet drag the resultant drag is less than the value obtained without blowing. Together with the increased lift due to blowing this gives values of the lift to drag ratio much higher than for the unblown case. Values of 13.8 and 18.7 were reached with C_{μ} values of 0.123 and 0.278 respectively.

5. In all the cases tested sideslip up to $\pm 5^{\circ}$ had no appreciable effect on lift, drag, or pitching moment.

6. Tests were made both with and without blowing at wind-speeds of 50 ft/sec. to 200 ft/sec. (Re of 0.8×10^6 to 3.2×10^6) and no appreciable Reynolds number effect was observed.

7. Upper surface pressure distributions were recorded both without blowing and with blowing from all edges for a range of incidence at four chordwise stations. The effects of blowing can be clearly seen :

   (i) Edge blowing increases the peak suctions at all chordwise stations but the effect is more pronounced at the forward stations where a powerful leading edge vortex already exists without blowing.

   (ii) Blowing moves the vortex core outboard, for instance at $\alpha = 25^{\circ}$ the suction peak moves from 65% to 80% of the semi-span.

(iii) (i) and (ii) together with tuft observations indicate a considerable increase in the size and strength of the leading edge vortex with blowing at constant incidence.

(iv) Without blowing the secondary separation can be seen as a region of constant pressure outboard of the main suction peak but is eliminated by the blowing as the entrainment due to the jet prevents the build-up of air in the region near the leading edge which normally gives rise to the secondary separation without blowing.

(v) Comparison with the Mangler and Smith theory for the unblown case gives good agreement for the vortex core position showing the importance of the secondary separation on the main vortex core position. It also indicates that the entrainment effect of the leading edge vortices on the upper surface pressure distribution is by no means negligible.

8. Tests have been made with various forms of asymmetric blowing and the results with slot blowing from one wing tip only are presented here. Appreciable gains in lift are still achieved, for example at 25° incidence with a C_{μ} of 0.12 the value of C_L is 1.14 compared with a value of 1.16 obtained with blowing from all edges. In this case however tip blowing results in a nose down pitching moment as most of the increased lift is generated on the rear part of the wing. This type of asymmetric blowing produces large rolling moments and it would seem possible to trim up to 4° of sideslip by this means.

6. Acknowledgements

The author is indebted to Mr. G. M. Lilley of the Aerodynamics Department for his advice and encouragement during the course of the present work and to Mr. D. Horn for his assistance with the tunnel programme. The computations were made by Miss R. Fuller.

7. References

1. Jones, R.T. — Properties of low aspect ratio pointed wings below and above the speed of sound. N.A.C.A. Report 835, 1946.

2. Weber, J. — Some effects of flow separation on slender delta wings. R.A.E. Tech.Note Aero.2425, 1955.

3. Williams, J., Alexander, A.J. — A preliminary note on a wind tunnel investigation of trailing edge flap blowing on a 5% thick 60° delta wing. A.R.C. Report 19,240, 1957.

4. Williams, J., Alexander, A.J. — Some exploratory jet-flap tests on a 60° delta wing. A.R.C. Report 19,140, 1957.

5. Smith, V.J., Simpson, G.J. — A preliminary investigation of the effect of a thin high velocity tip jet on a low aspect ratio wing. Aust. Dept. of Supply Note A.R L. A.163, 1957.

6. Ayers, R.F., Wilde, M.R. — Aerodynamic characteristics of a swept wing with spanwise blowing. College of Aeronautics Note 57, 1956.

7. Harris, K.D. — Unpublished note.

8. Squire, L.C., Capps, D.S. — Experimental investigation of the characteristics of an ogee wing from M = 0.4 to M = 1.8. R.A.E. Tech. Note Aero 2648, 1959.

9. Peckham, D.H. — Low speed wind tunnel tests on a series of uncambered slender pointed wings. R.A.E. Report Aero 2613, 1958.

10. Marsden, D.J., Simpson, R.W., Rainbird, W.E. — An investigation into the flow over delta wings at low speeds with leading edge separation. College of Aeronautics Report 114, 1958.

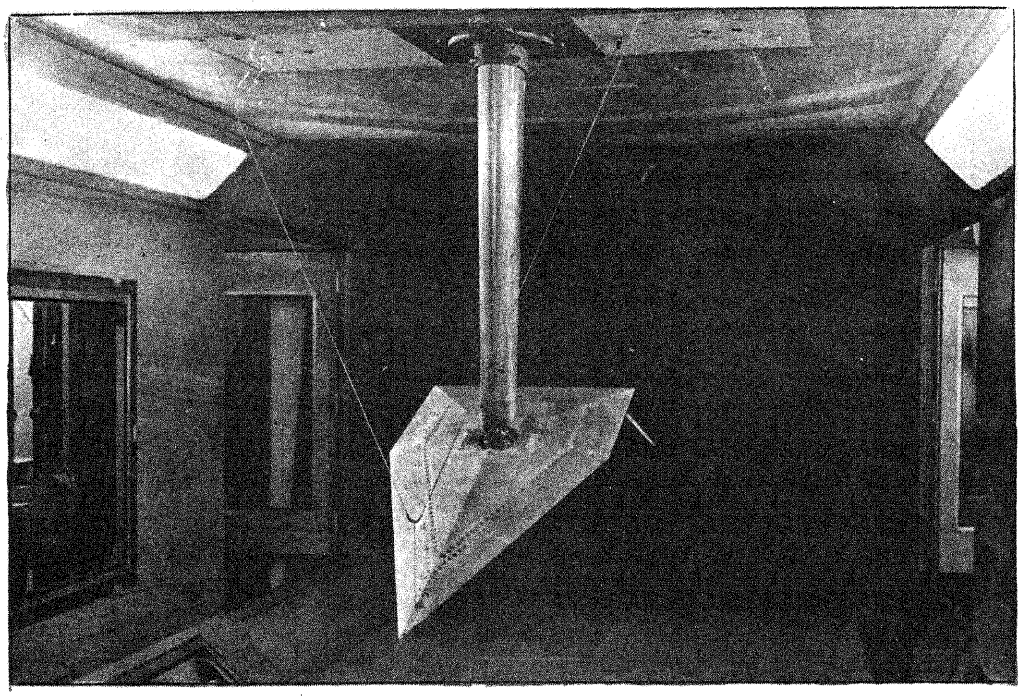

FIG. 1. MODEL MOUNTED IN WIND TUNNEL

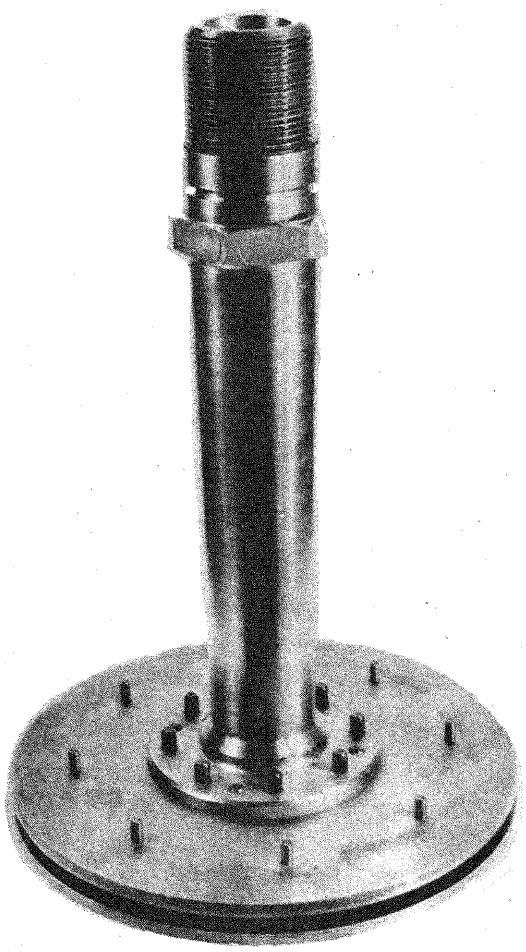

FIG. 2. THE CALIBRATOR

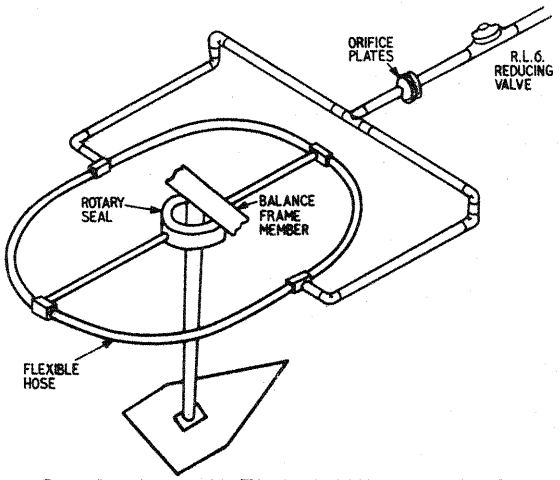

FIG. 3. MODEL MOUNTING SHOWING FLEXIBLE RING MAIN.

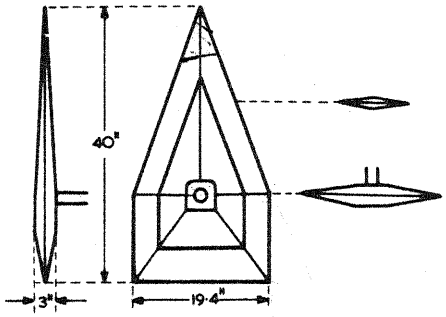

FIG. 4. DIAGRAM OF MODEL.

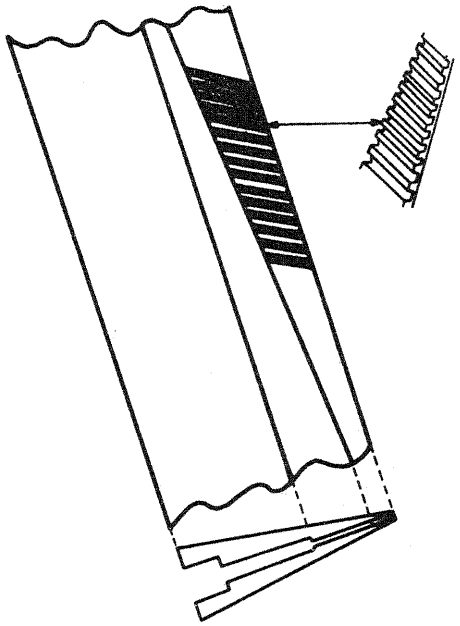

FIG. 5. EDGE SLOTS FOR DIRECTING AND TAPERING THE JET SHEET

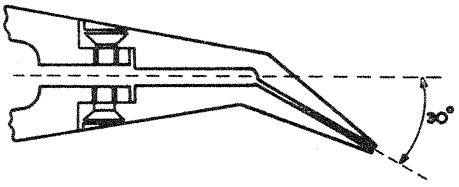

FIG. 6. 30° DROOPED EDGE.

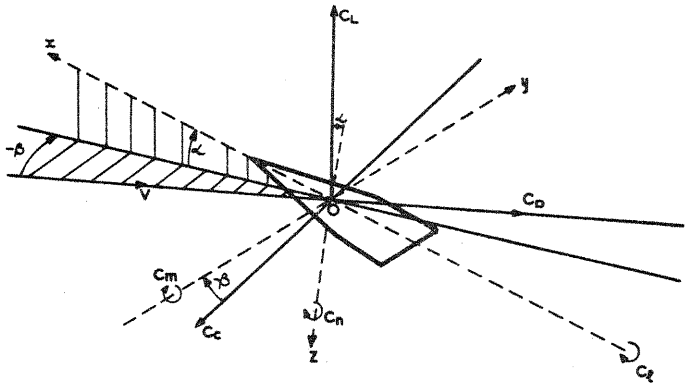

FIG. 7 FORCE AND MOMENT AXES SYSTEM.

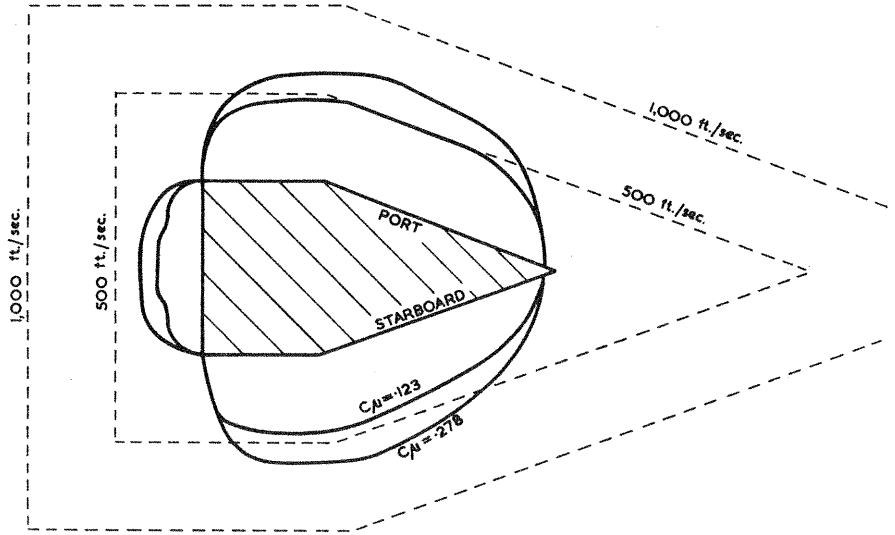

FIG. 8. SLOT VELOCITY DISTRIBUTION WITH BLOWING FROM ALL EDGES.

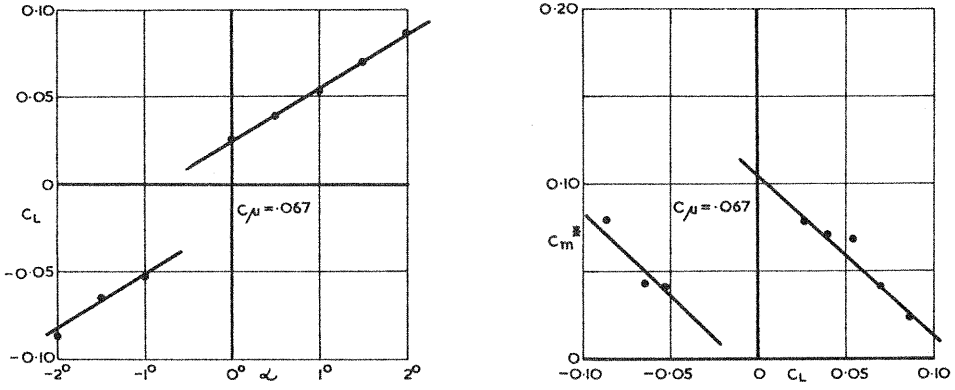

FIG. 9. JET SHEET INSTABILITY NEAR ZERO INCIDENCE WITH BLOWING FROM ALL EDGES.

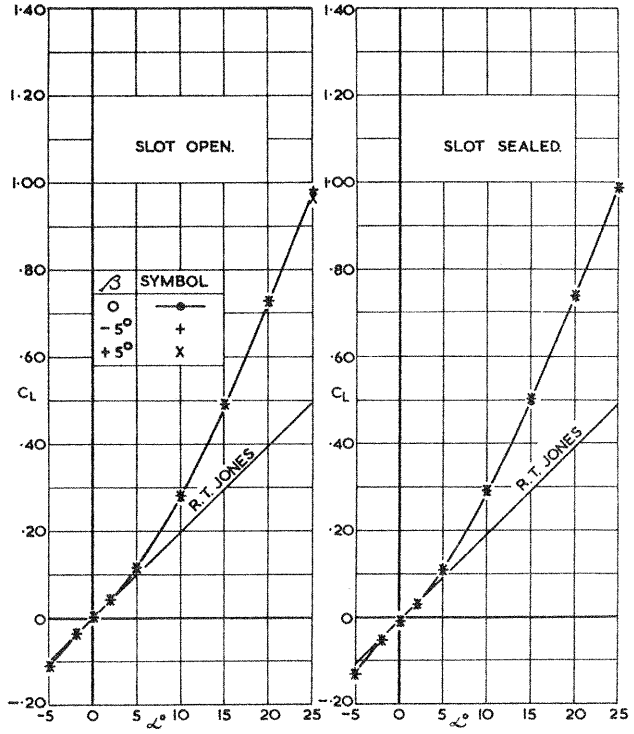

FIG. 10. VARIATION OF LIFT WITH INCIDENCE, $C_\mu = 0$

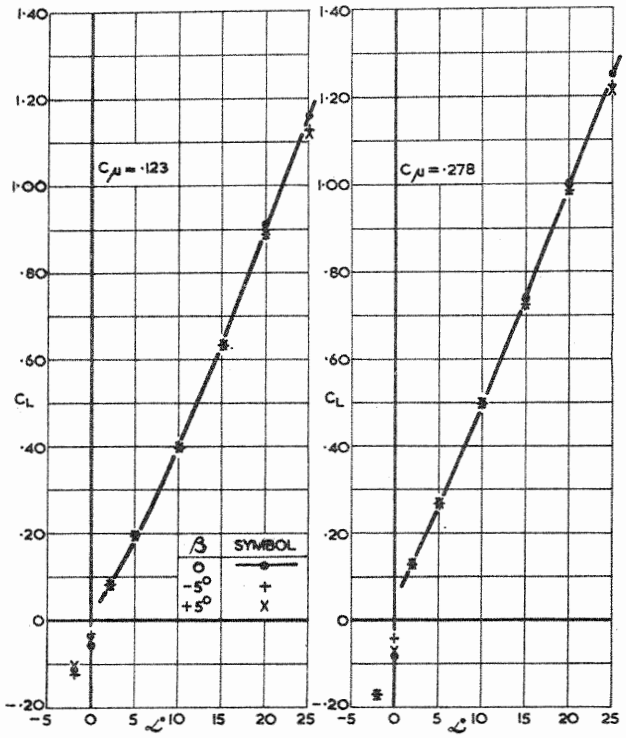

FIG. 11. VARIATION OF LIFT WITH INCIDENCE. BLOWING FROM ALL EDGES.

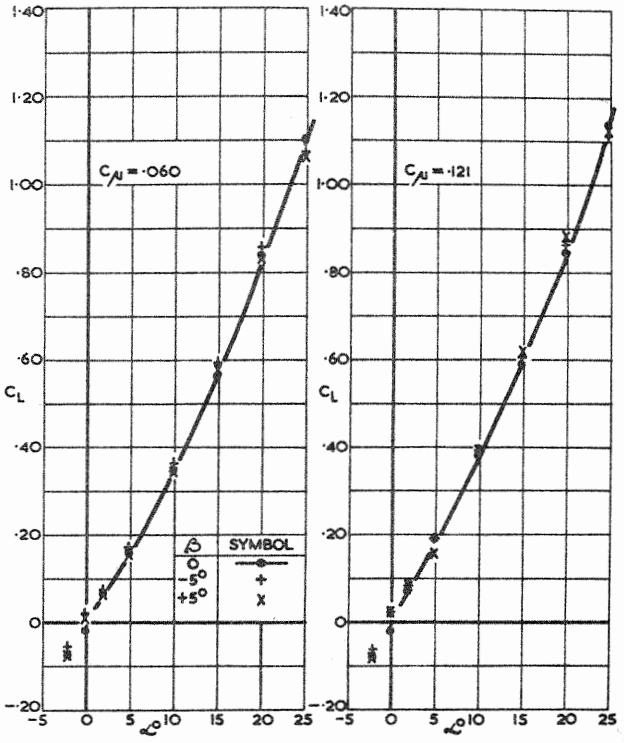

FIG. 12. VARIATION OF LIFT WITH INCIDENCE. BLOWING FROM STARBOARD TIP

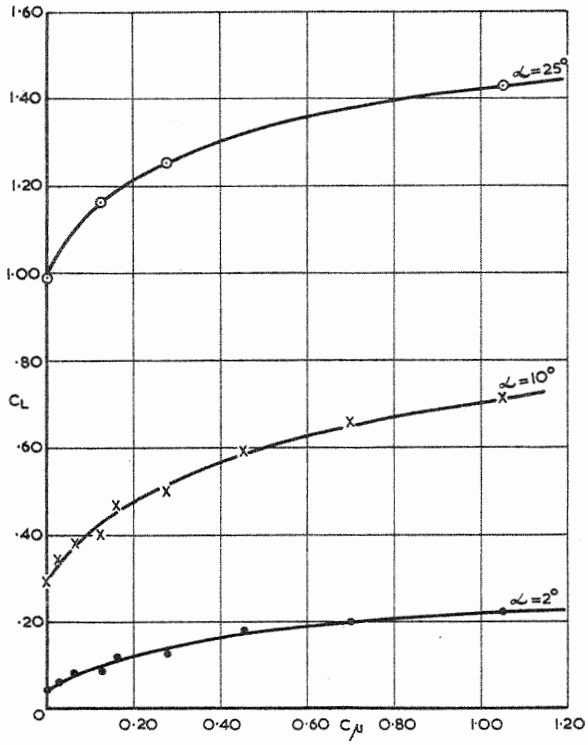

FIG. 13. VARIATION OF LIFT WITH MOMENTUM COEFFICIENT AT CONSTANT INCIDENCE. BLOWING FROM ALL EDGES.

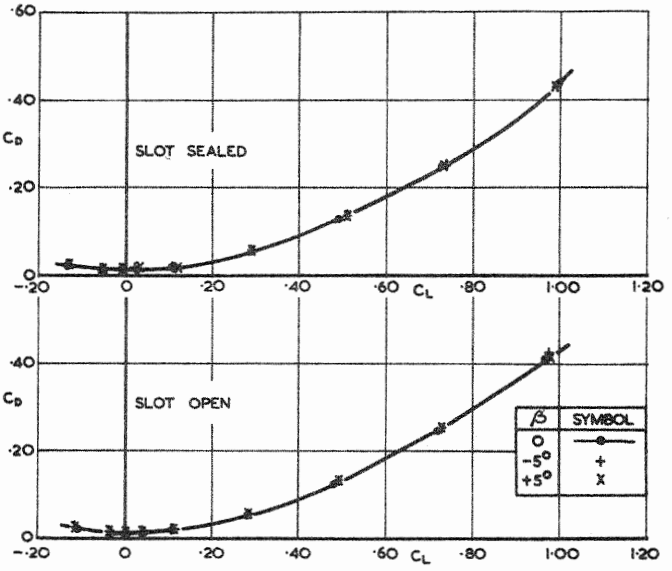

FIG. 14. VARIATION OF DRAG WITH LIFT.
$C_\mu = 0$

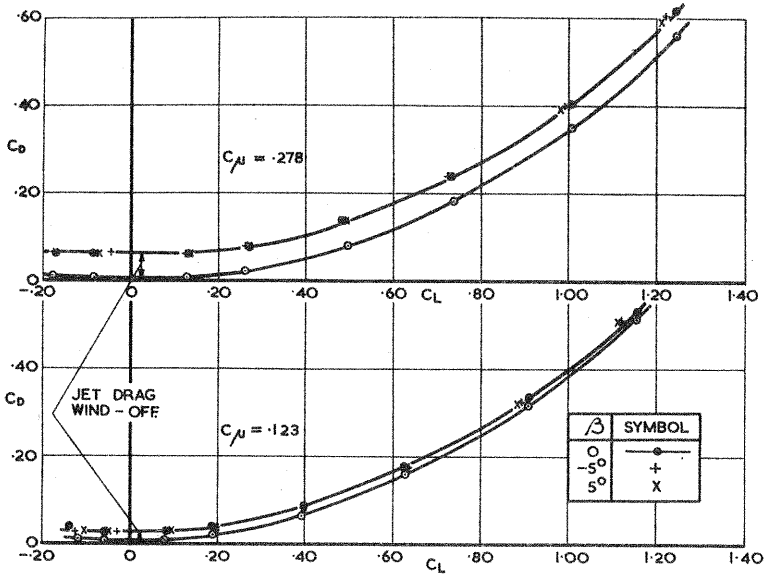

FIG. 15. VARIATION OF DRAG WITH LIFT.
BLOWING FROM ALL EDGES.

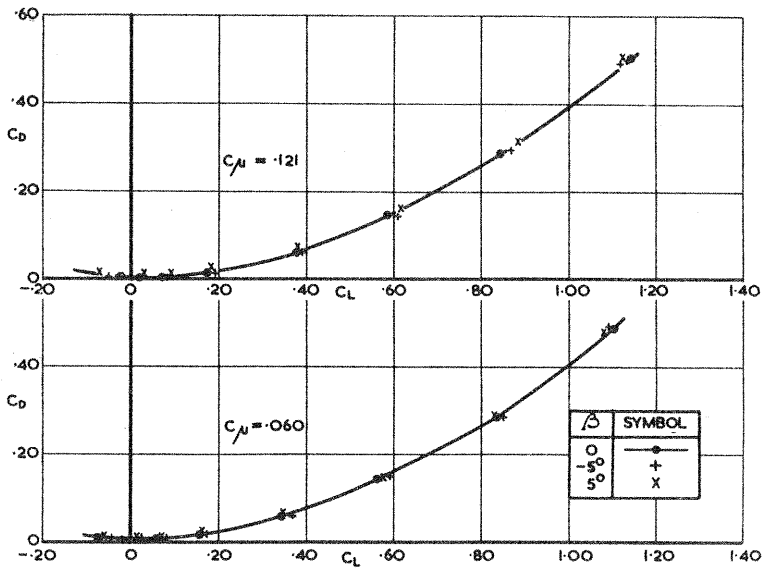

FIG. 16. VARIATION OF DRAG WITH LIFT.
BLOWING FROM STARBOARD TIP.

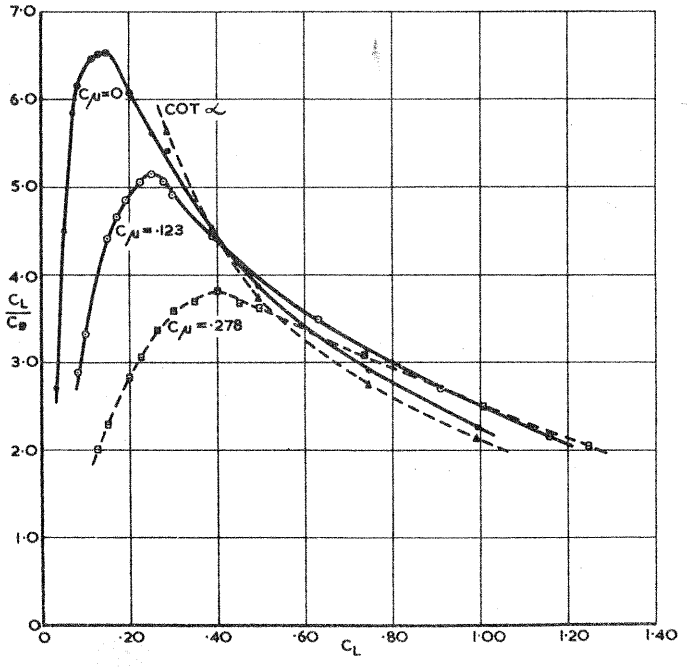

FIG. 17a. VARIATION OF C_L/C_D WITH LIFT.
C_μ = 0 AND BLOWING FROM ALL EDGES.

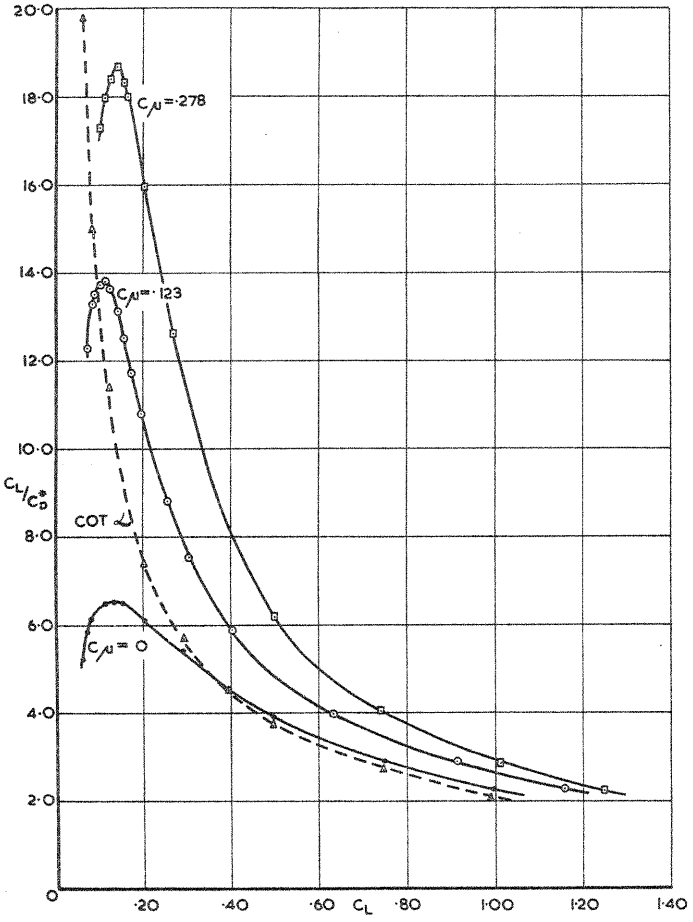

FIG. 17b. VARIATION OF C_L/C_D^* WITH LIFT. $C_\mu = 0$ AND BLOWING FROM ALL EDGES.

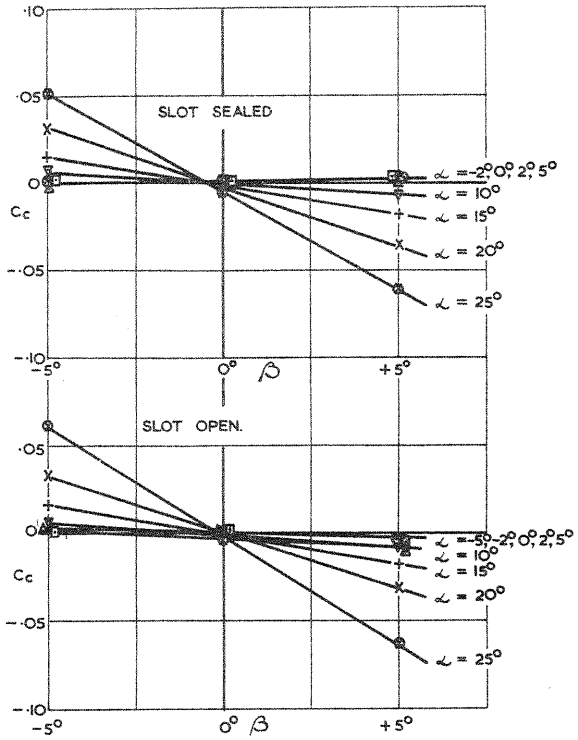

FIG. 18. VARIATION OF CROSSWIND FORCE WITH SIDESLIP ANGLE β $C_\mu = 0$

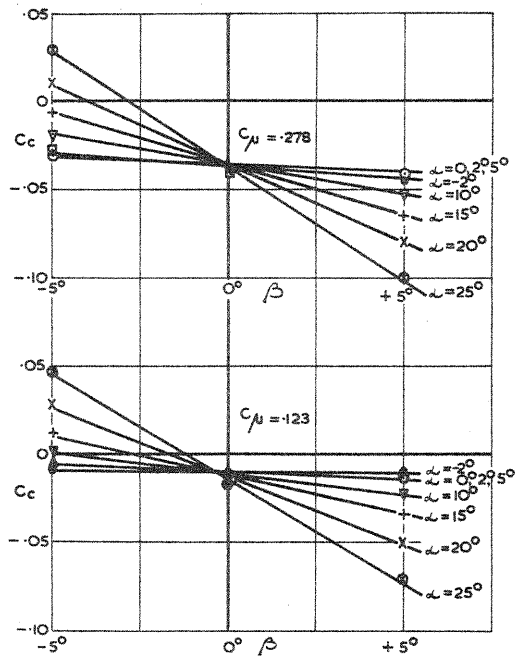

FIG. 19. VARIATION OF CROSSWIND FORCE WITH SIDESLIP ANGLE β BLOWING FROM ALL EDGES

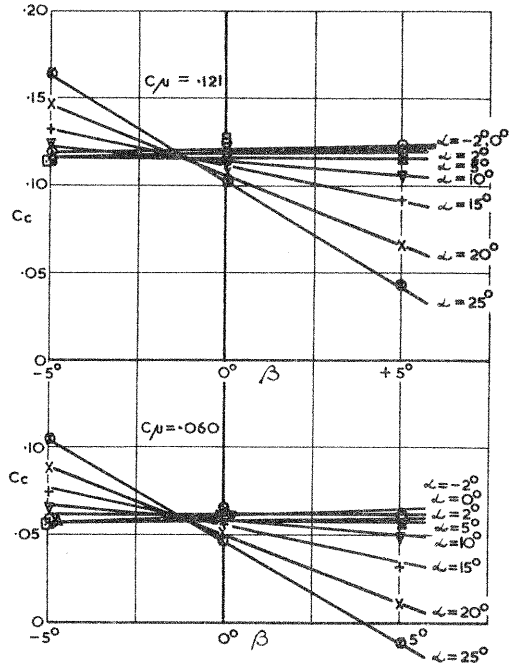

FIG. 20. VARIATION OF CROSSWIND FORCE WITH SIDESLIP ANGLE β BLOWING FROM STARBOARD TIP

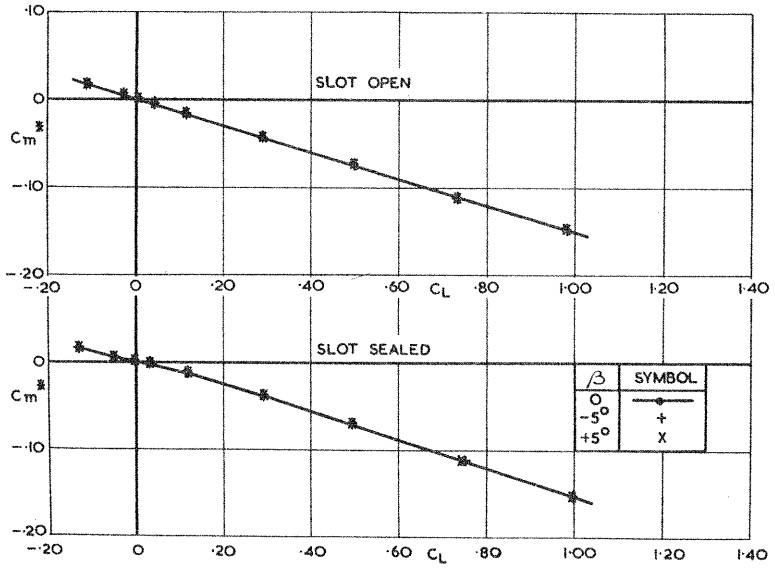

FIG. 21. VARIATION OF PITCHING MOMENT WITH LIFT. $C_\mu = 0$

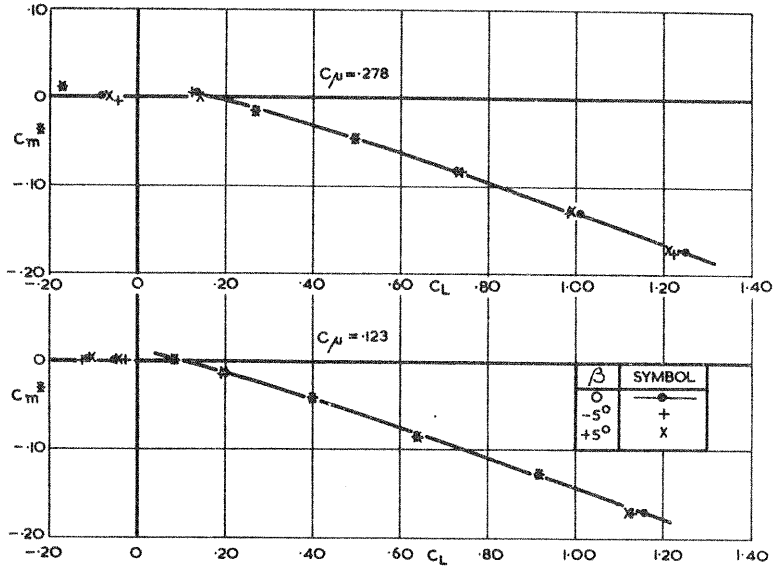

FIG. 22. VARIATION OF PITCHING MOMENT WITH LIFT BLOWING FROM ALL EDGES.

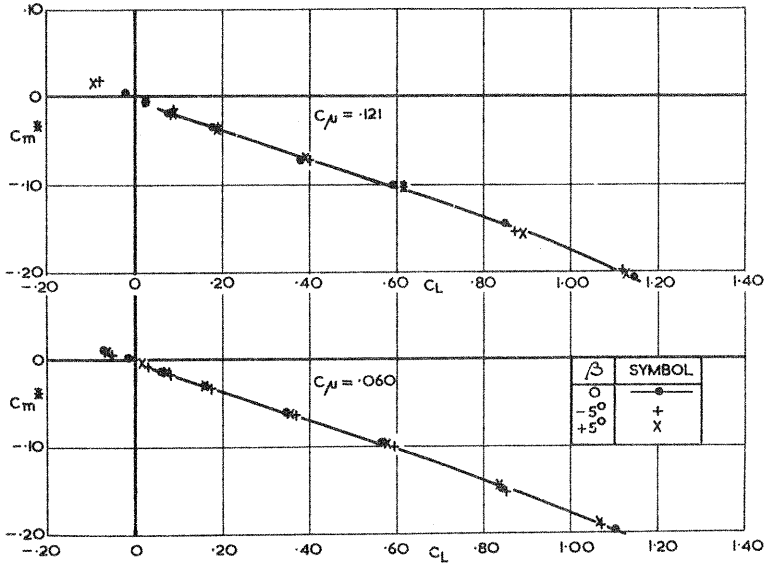

FIG. 23. VARIATION OF PITCHING MOMENT WITH LIFT BLOWING FROM STARBOARD TIP.

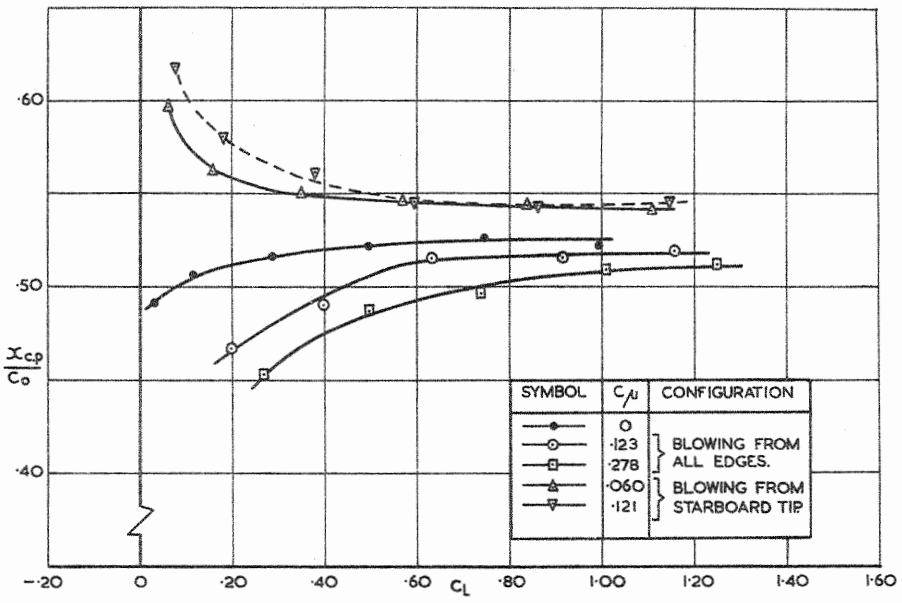

FIG. 24. MOVEMENT OF CENTRE OF PRESSURE WITH LIFT.

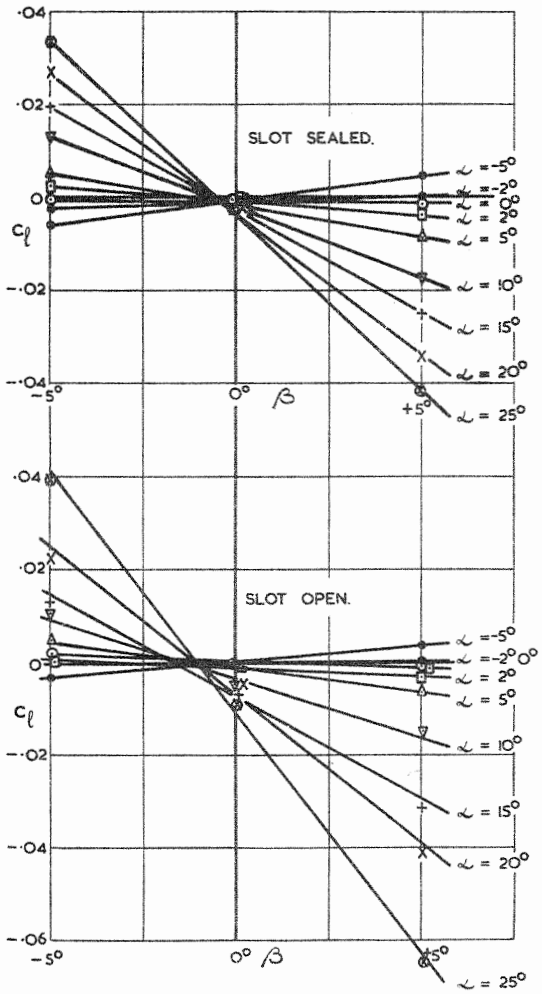

FIG. 25. VARIATION OF ROLLING MOMENT WITH SIDESLIP ANGLE β $C_{\mu}=0$

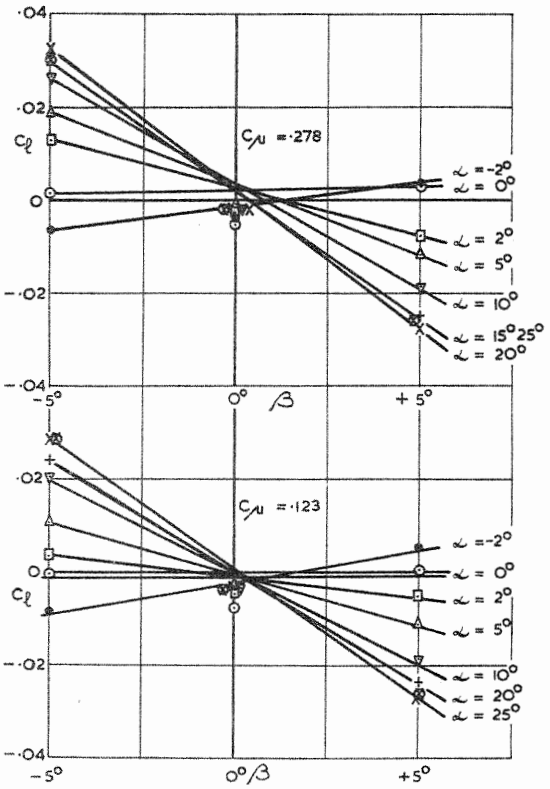

FIG. 26. VARIATION OF ROLLING MOMENT WITH SIDESLIP ANGLE β BLOWING FROM ALL EDGES

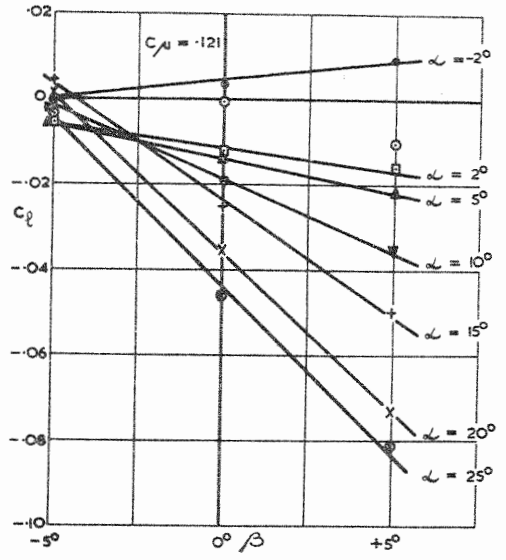

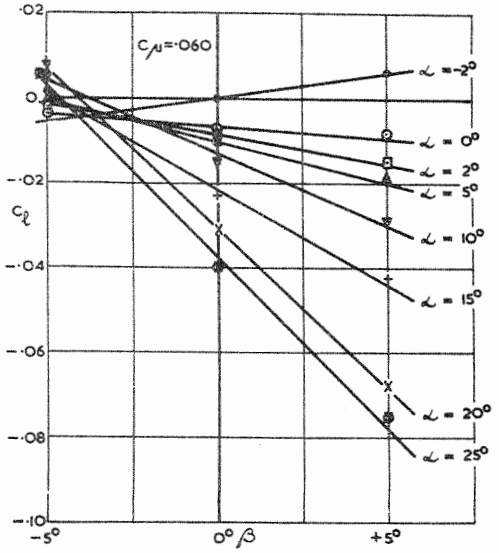

FIG. 27. VARIATION OF ROLLING MOMENT WITH SIDESLIP ANGLE β BLOWING FROM STARBOARD TIP.

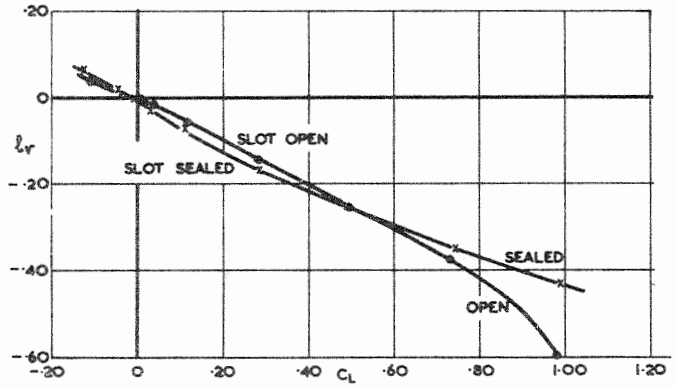

FIG. 28. VARIATION OF $l_v \left(\equiv \frac{\partial C_l}{\partial \beta}\right)$ WITH LIFT.

$C_{\mu} = 0$

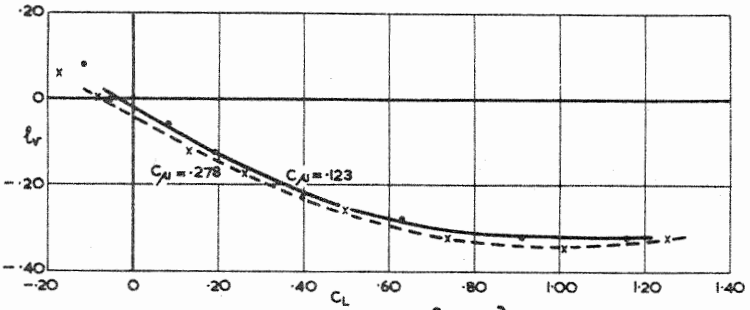

FIG. 29. VARIATION OF $l_v \left(\equiv \frac{\partial C_l}{\partial \beta}\right)$ WITH LIFT BLOWING FROM ALL EDGES.

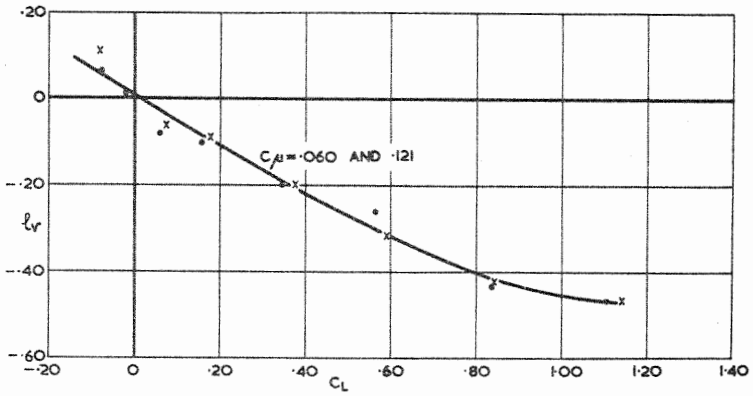

FIG. 30. VARIATION OF $l_v \left(\equiv \frac{\partial C_l}{\partial \beta}\right)$ WITH LIFT BLOWING FROM STARBOARD TIP.

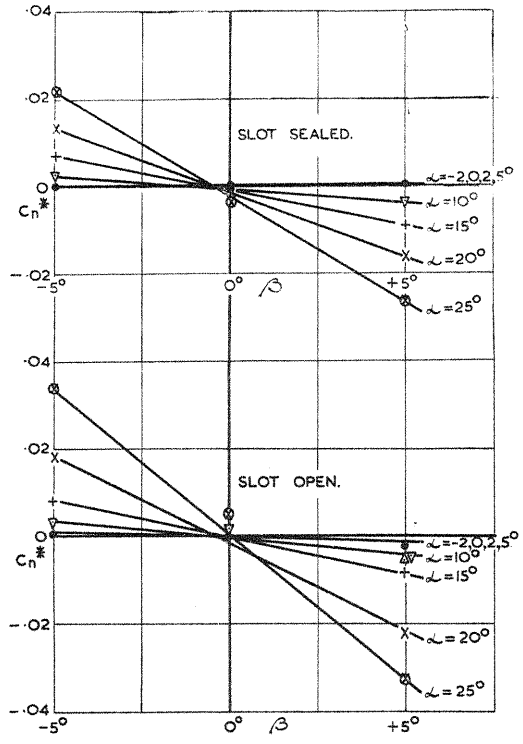

FIG. 31. VARIATION OF YAWING MOMENT WITH SIDESLIP ANGLE β $C_\mu = 0$

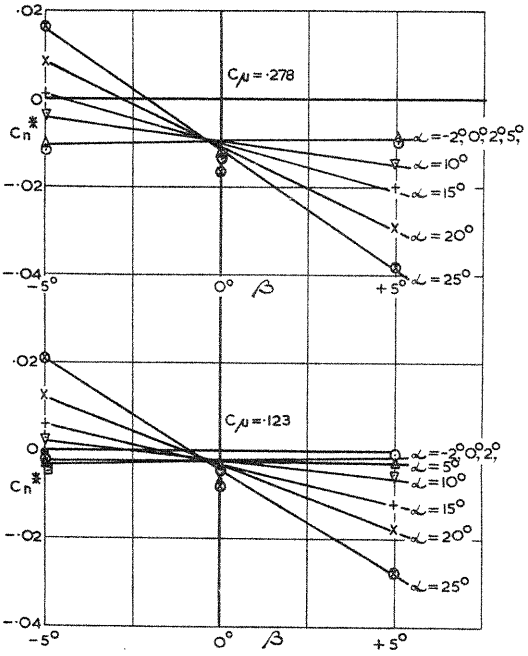

FIG. 32. VARIATION OF YAWING MOMENT WITH SIDESLIP ANGLE β BLOWING FROM ALL EDGES.

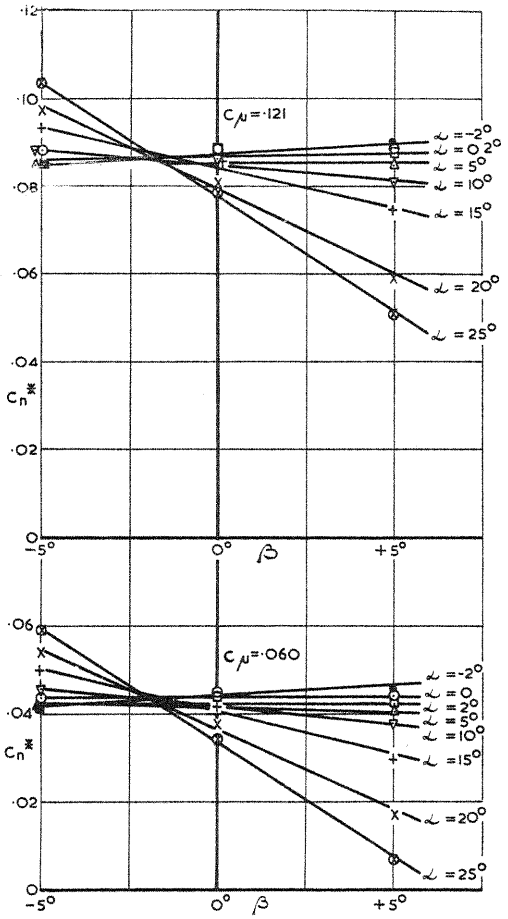

FIG. 33. VARIATION OF YAWING MOMENT WITH SIDESLIP ANGLE β BLOWING FROM STARBOARD TIP

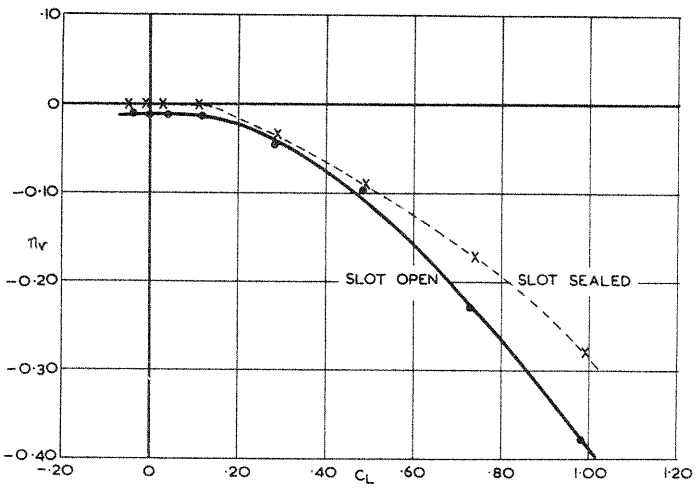

FIG. 34. VARIATION OF $\eta_v \left(\equiv \frac{\partial C_n^*}{\partial \beta}\right)$ WITH LIFT.

$C_\mu = 0$

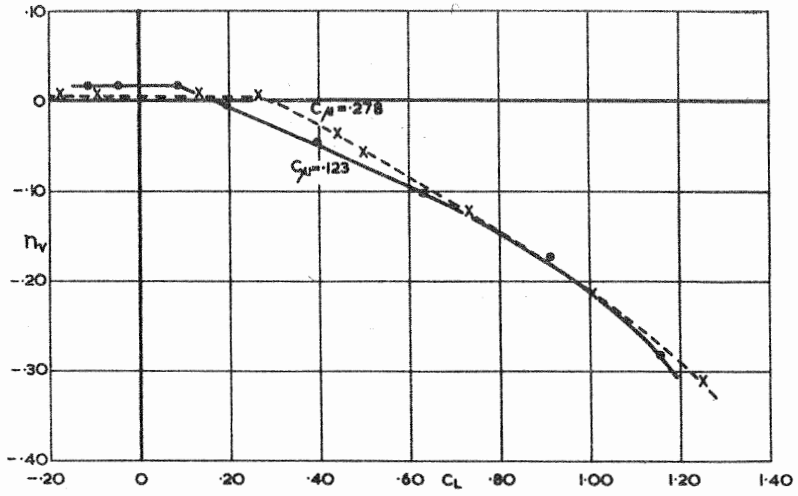

FIG. 35. VARIATION OF $n_v \left(\equiv \frac{\partial C_n^*}{\partial \beta}\right)$ WITH LIFT.

BLOWING FROM ALL EDGES.

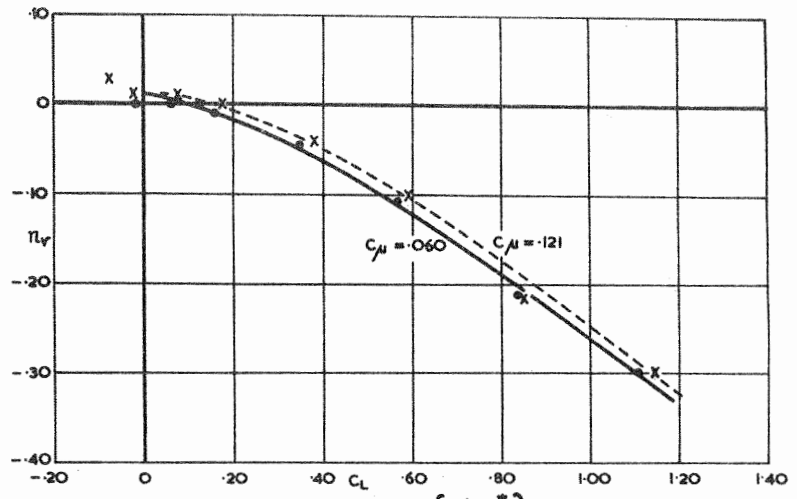

FIG. 36. VARIATION OF $n_v \left(\equiv \frac{\partial C_n^*}{\partial \beta}\right)$ WITH LIFT.

BLOWING FROM STARBOARD TIP.

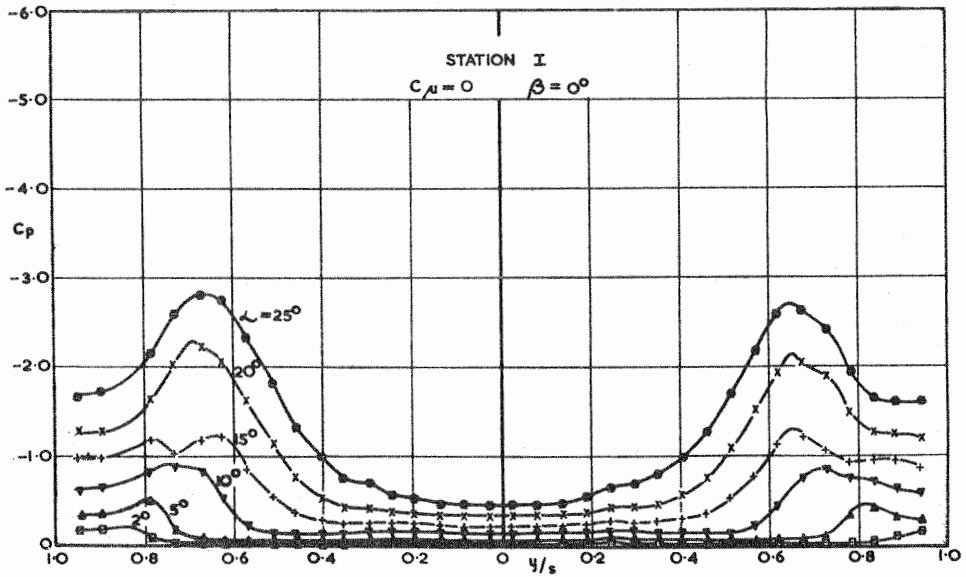

FIG. 37. UPPER SURFACE PRESSURE DISTRIBUTION $x'/c_0 = 0 \cdot 33$

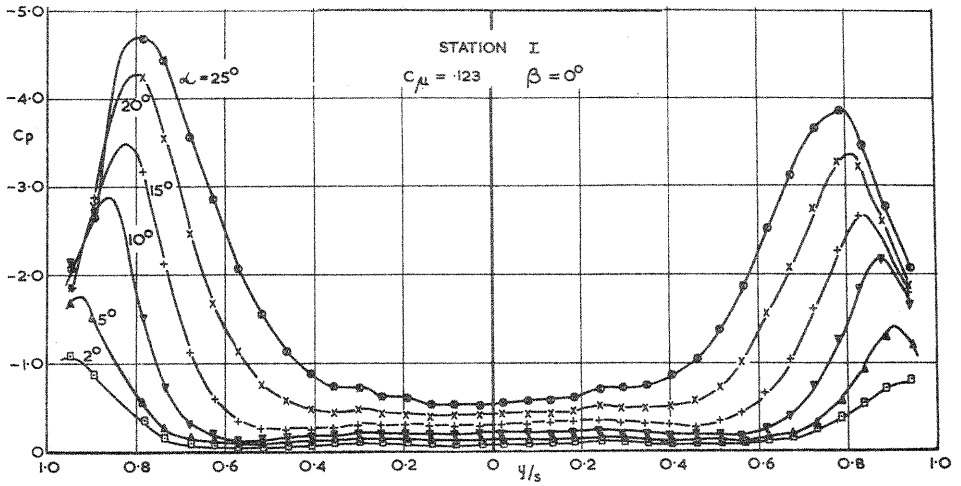

FIG. 38. UPPER SURFACE PRESSURE DISTRIBUTION $x'/c_0 = 0.33$
BLOWING FROM ALL EDGES.

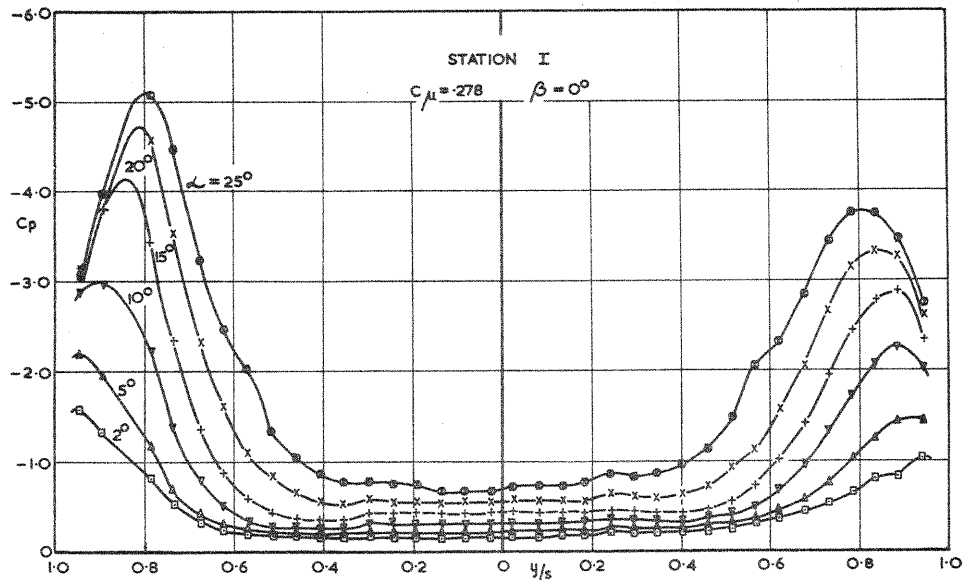

FIG. 39. UPPER SURFACE PRESSURE DISTRIBUTION $x'/c_0 = 0.33$
BLOWING FROM ALL EDGES.

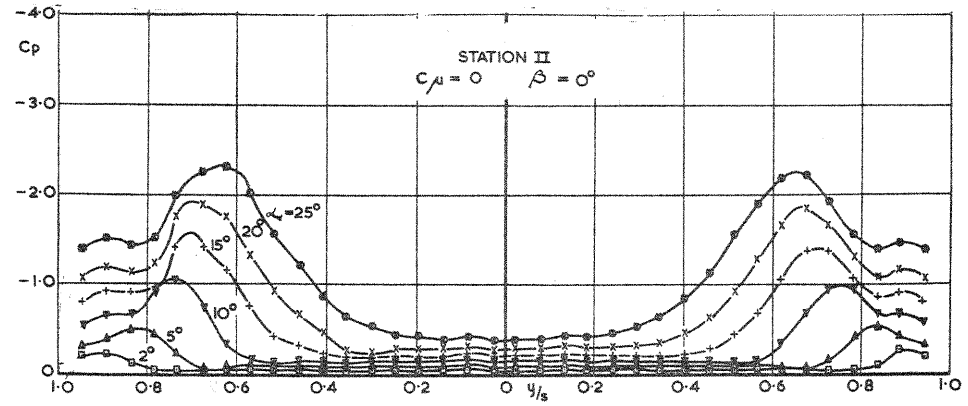

FIG. 40. UPPER SURFACE PRESSURE DISTRIBUTION $x'/c_0 = 0.49$

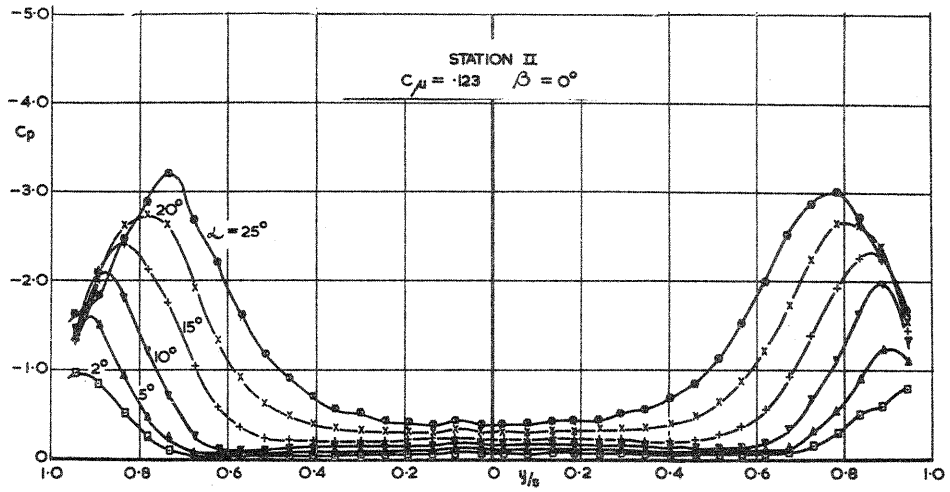

FIG. 41. UPPER SURFACE PRESSURE DISTRIBUTION $x'/C_0 = 0{\cdot}49$
BLOWING FROM ALL EDGES.

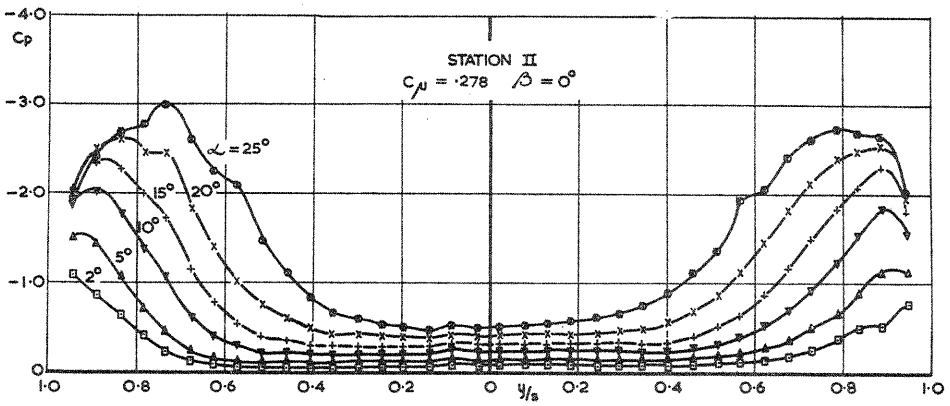

FIG. 42. UPPER SURFACE PRESSURE DISTRIBUTION $x'/C_0 = 0{\cdot}49$
BLOWING FROM ALL EDGES.

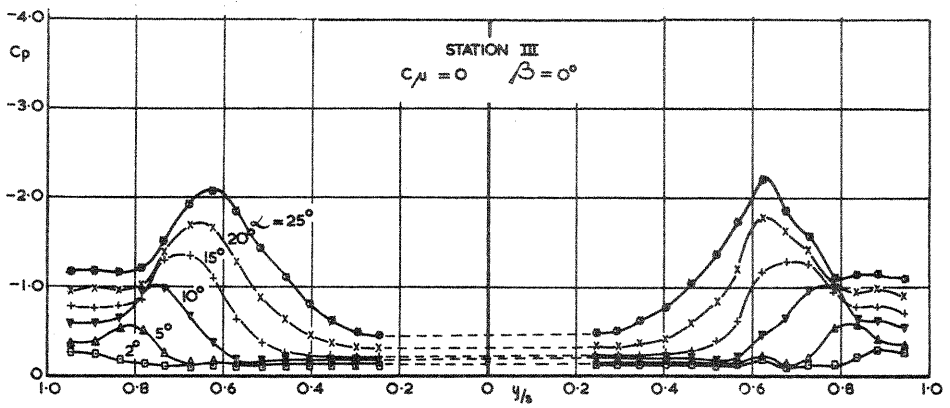

FIG. 43. UPPER SURFACE PRESSURE DISTRIBUTION $x'/C_0 = 0{\cdot}63$

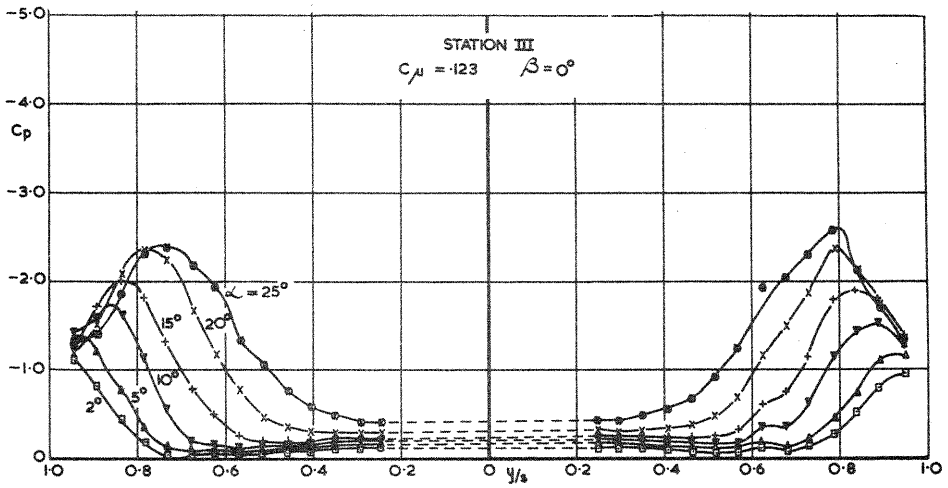

FIG. 44. UPPER SURFACE PRESSURE DISTRIBUTION $x'/c_0 = 0{\cdot}63$
BLOWING FROM ALL EDGES.

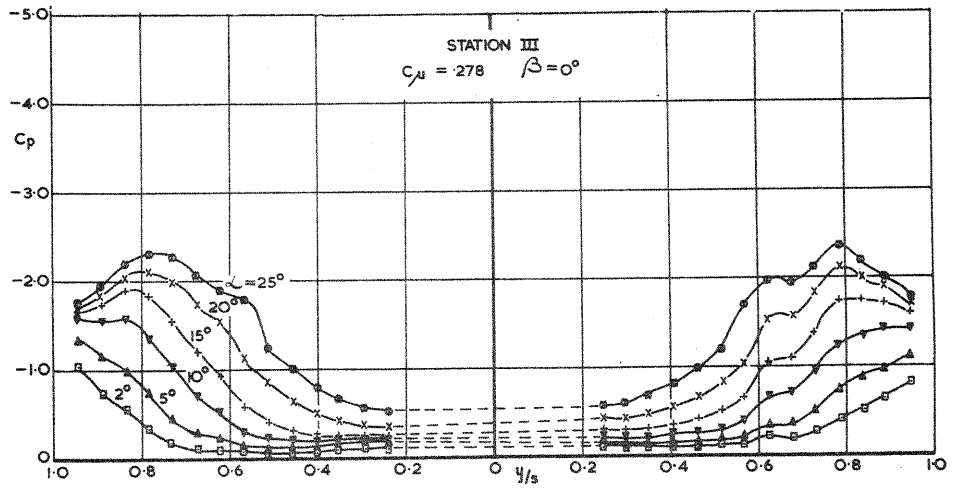

FIG. 45. UPPER SURFACE PRESSURE DISTRIBUTION $x'/c_0 = 0{\cdot}63$
BLOWING FROM ALL EDGES.

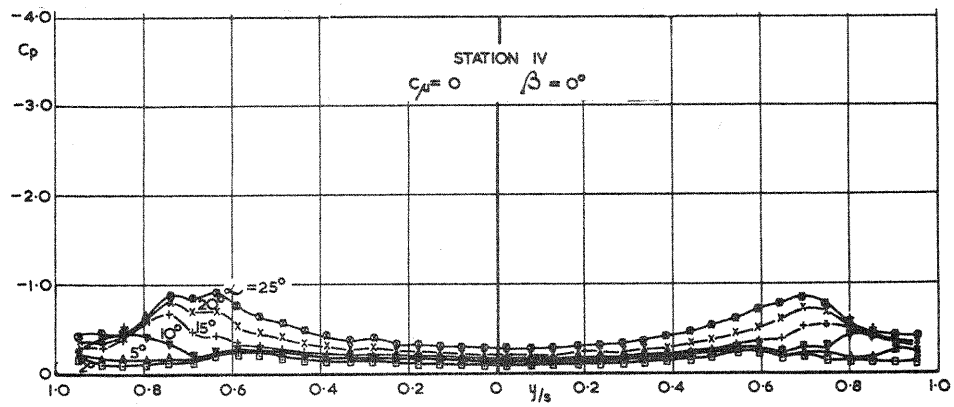

FIG. 46. UPPER SURFACE PRESSURE DISTRIBUTION $x'/c_0 = 0{\cdot}87$

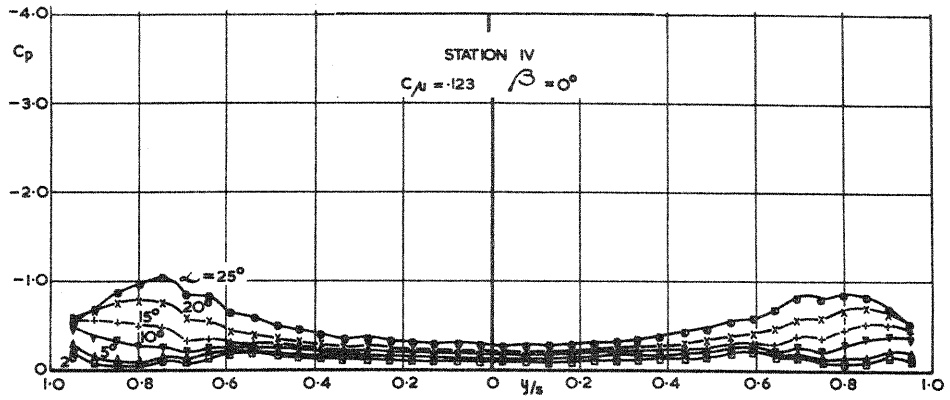

FIG. 47. UPPER SURFACE PRESSURE DISTRIBUTION $x'/C_0 = 0.87$
BLOWING FROM ALL EDGES.

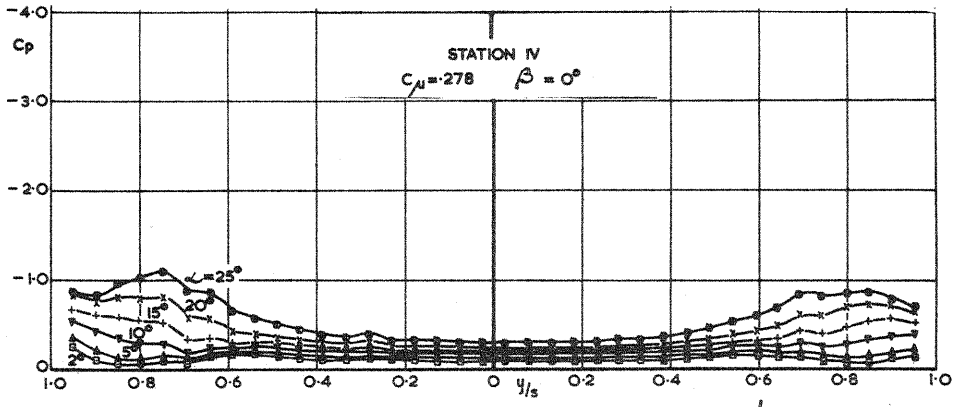

FIG. 48. UPPER SURFACE PRESSURE DISTRIBUTION $x'/C_0 = 0.87$
BLOWING FROM ALL EDGES

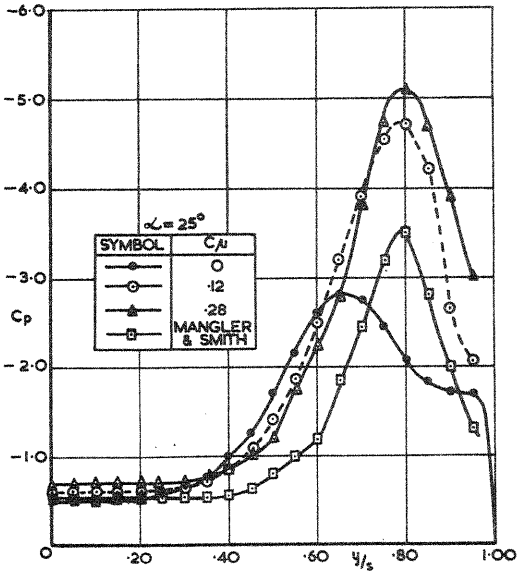

FIG. 49. UPPER SURFACE PRESSURE DISTRIBUTION
$x'/C_0 = 0.33$ COMPARISON WITH THEORY.